

XBeach BOI - Approaches to reduce calculation time



XBeach BOI - Approaches to reduce calculation time

Author(s)

Roel de Goede
Menno de Ridder
Ellen Quataert
Robert McCall

Project context (EN/NL)

This report is part of the project “Plan Zandige Waterkeringen” (Plan for Sandy Coastal Defences), which is financed by the Ministry of Infrastructure and Water Management of the Netherlands, Rijkswaterstaat, STOWA, Waterschap Scheldestromen, Waterschap Hollandse Delta, Hoogheemraadschap van Delfland, Hoogheemraadschap van Rijnland, Hoogheemraadschap Hollands Noorderkwartier and Wetterskip Fryslân. The “Plan Zandige Waterkeringen” project aims to develop a new instrument to manage, assess and design sandy coastal defences. The project is part of the BOI-program.

Dit rapport is onderdeel van het project Plan Zandige Waterkeringen. Plan Zandige Waterkeringen wordt gefinancierd door het Ministerie van Infrastructuur en Waterstaat, Rijkswaterstaat, STOWA, Waterschap Scheldestromen, Waterschap Hollandse Delta, Hoogheemraadschap van Delfland, Hoogheemraadschap van Rijnland, Hoogheemraadschap Hollands Noorderkwartier en het Wetterskip Fryslân. Dit project richt zich op de vernieuwing van het instrumentarium ten behoeve van het beheren, beoordelen en ontwerpen van zandige waterkeringen. Het project Plan Zandige Waterkeringen maakt deel uit van het programma BOI (Beoordelings- en Ontwerpinstrumentarium).

XBeach BOI - Approaches to reduce calculation time

Client	Rijkswaterstaat Water, Verkeer en Leefomgeving
Contact	de heer R. Wilmink
Client project leader	Rinse Wilmink (Project leader "Plan Zandige Waterkeringen")
Client review by	Rinse Wilmink, Niels van Kuik
Reference	Plan van Aanpak Vernieuwd Instrumentarium Zandige Keringen, 11203720-014-GEO-0001
Keywords	Safety assessment, BOI, XBeach, dune erosion, calculation time, morfac, directional spreading

Document control

Version	1.0
Date	29-04-2021
Project nr.	11205758-029
Document ID	11205758-029-GEO-0012
Pages	68
Classification	
Status	final

Author(s)

	Roel de Goede	
	Menno de Ridder	
	Ellen Quataert	
	Robert McCall	

Doc. version	Author	Reviewer	Approver	Publish
1.0	Roel de Goede	Ap van Dongeren	Jan Aart van Twillert	
	Menno de Ridder			
	Ellen Quataert			
	Robert McCall			

Summary

A summary in Dutch is provided on the next page.

As part of the BOI (“Beoordeling en Ontwerp Instrumentarium”) program, Deltares is developing a new national dune safety assessment methodology as set out in the Action Plan for the Safety Assessment of Sandy Coasts (“*Plan van Aanpak Vernieuwd Instrumentarium Zandige Keringen*”, in Dutch; Deltares/Arcadis, 2019a). This report concerns one of the steps required for this development, relating to the application of the process-based dune erosion model XBeach. The objective of the current study is to investigate possible approaches that result in a significant reduction in computational time for the dune safety assessment of 2023, with limited compromise in model accuracy and consistency.

Four approaches to reduce calculation time have been investigated. The first is to facilitate the application of a 1D (cross-shore) modelling approach for alongshore-uniform situations. Due to the simplifications inherent in all wave-resolving cross-shore models, including wave flume experiments, 1D XBeach models overestimate infragravity wave growth and subsequent dune erosion volumes. These simplifications and subsequent overestimations are not present in 2DH (area) models. To ensure 1D XBeach models provide an accurate representation of infragravity wave dynamics and dune erosion along the Dutch coast, a parameterization was developed to mimic 2DH infragravity dynamics in a 1D XBeach models. This approach subsequently greatly reduces the difference in dune erosion predicted by 1D and 2DH XBeach models from a relative bias of 56% to less than 2%. The gain in computational time using this ‘modified 1D approach’ compared to a 2DH approach, which would otherwise be required for accurate simulation of dune erosion, is significant, with computational times reduced on average by a factor 60.

Using the modified 1D approach, three additional approaches are investigated that provide a significant reduction in computational time with only a small loss in model consistency: applying a morphological acceleration factor (*morfac*), optimizing the location of the minimum grid resolution, and increasing the computational time step. The combination of these three approaches (the accelerated modified 1D approach) showed a further reduction in computational time by a factor ~10.

Altogether, the accelerated modified 1D approach provides a reduction in computational time of a factor 500 on average, which is the combined effect of a modified 1D approach with respect to 2DH (factor ~60) and the accelerations to the modified 1D approach (factor ~10). The results of the modified 1D approach are consistent with the 2DH-based approach, with a deviation in the dune erosion volume of, on average, less than 3%.

Mean computation times for the 1D-based approach on a standard workstation computer are approximately 7 minutes if an entire storm (32 hours) is simulated, or approximately 2 minutes if only maximum storm conditions are simulated, as is currently the case in the dune safety assessment methodology. While computation times are longer than those in the current safety assessment methodology (which is an empirical model), they are manageable and sufficiently short to allow for the development of the probabilistic and semi-probabilistic models required in Phase 1 and 2 of the *BOI Zandige Waterkeringen* project.

Samenvatting

Binnen het BOI-project ("Beoordeling en Ontwerp Instrumentarium") ontwikkelt Deltares een nieuw instrumentarium voor de veiligheidsbeoordeling van de Nederlandse duinenkust, zoals voorgesteld in het Plan van Aanpak Vernieuwd Instrumentarium Zandige Keringen (Deltares/Arcadis, 2019a). Dit rapport beschrijft de uitvoering en resultaten van één van de benodigde ontwikkelingsstappen van het nieuwe instrumentarium met betrekking tot gebruik van het proces-gebaseerde duinerosiemodel XBeach. Het doel van de huidige studie is om mogelijke methoden te onderzoeken die resulteren in een significante verkorting van de rekentijd van het instrumentarium, met een beperkte afname in modelnauwkeurigheid en consistentie.

In deze studie zijn vier benaderingen onderzocht om de rekentijd te verkorten. De eerste betreft het ontwikkelen van een nauwkeurige en consistente ééndimensionale (1D; kustdwars profiel) modelaanpak voor langs-uniforme kusten. Door versimpelingen in 1D golfplossende modellen, inclusief fysische modellen in een golfgoot, worden lange golven overschat ten opzichte van de werkelijkheid, waardoor duinerosie ook overschat wordt. Deze overschatting vindt niet plaats in twee-dimensionale (2DH; gebieds-) modellen. Binnen deze studie is een methode ontwikkeld om de lange golf dynamica van 2DH XBeach modellen in 1D modellen na te bootsen. Hierdoor wordt het relatieve verschil tussen de berekende duinerosie in een 1D en 2DH modelaanpak sterk verkleind van 56% tot minder dan 2%. De winst in rekentijd met behulp van deze "aangepaste 1D-benadering" in vergelijking met een 2DH-benadering, die anders nodig zou zijn voor een nauwkeurige beoordeling, is gemiddeld een factor 60.

Met behulp van de aangepaste 1D-benadering zijn er drie aanvullende methoden gevonden die een aanzienlijke vermindering van de rekentijd en een klein verlies aan consistentie opleveren: het toepassen van een morfologische versnellingsfactor (*morfac*), het optimaliseren van de locatie van de minimale resolutie in het rekenrooster, en het vergroten van de tijdstap. De combinatie van deze drie methoden (de versnelde aangepaste 1D-benadering) toonde een verdere vermindering van de rekentijd met een factor ~ 10.

Gezamenlijk leiden de versnellingsmethoden tot een vermindering van de rekentijd met gemiddeld een factor 500, wat het gecombineerde effect is van een aangepaste 1D-benadering ten opzichte van 2DH (factor ~ 60) en de versnellingen naar de aangepaste 1D-benadering (factor ~ 10). De resultaten van de aangepaste 1D-benadering zijn consistent met de 2DH-benadering, met een gemiddeld verschil in duinerosie van minder dan 3%.

Gemiddelde reketijden voor de 1D-benadering op een standaard rekencomputer zijn ongeveer 7 minuten als een hele storm (32 uur) wordt gesimuleerd, of ongeveer 2 minuten als alleen maximale stormcondities worden gesimuleerd, zoals het geval is in de huidige methodologie voor veiligheidsbeoordeling zandige keringen. Hoewel de reketijden langer zijn dan die in de huidige methodologie voor veiligheidsbeoordeling (een empirisch model), zijn ze beheersbaar en voldoende kort om de ontwikkeling van de probabilistische en semi-probabilistische modellen mogelijk te maken die vereist zijn in Fase 1 en 2 van het BOI Zandige Waterkeringen project.

Contents

	Summary	4
	Samenvatting	5
1	Introduction	8
1.1	Background	8
1.1.1	General	8
1.1.2	Current subproject	8
1.2	Research questions	9
1.3	Outline	9
2	Approach	10
2.1	General approach	10
2.2	Input data	11
2.2.1	Cross-shore profiles	11
2.2.2	Forcing conditions	14
2.3	Model set-up of the base case	16
2.3.1	Model grid	16
2.3.2	Model settings	17
2.4	Morphological indicators	18
2.5	Evaluation measures	19
2.6	Effect of random wave seeding on dune erosion volumes	19
3	Including the effects of directional spreading in a 1D XBeach approach	20
3.1	Introduction	20
3.2	Implementation	20
3.3	Calibration	21
3.3.1	Setup	21
3.3.2	Results	22
3.3.3	Optimal alpha-E	26
3.4	Validation	29
3.5	Conclusions	33
4	Morphological acceleration factor ‘<i>morfac</i>’	35
4.1	Introduction	35
4.2	Approach	35
4.3	Results	36
4.3.1	Constant boundary conditions	36
4.3.2	Time-varying boundary conditions	40
4.4	Conclusion	42

5	Grid resolution and timestep	43
5.1	Introduction	43
5.2	Minimum cross-shore grid size 'dxmin'	43
5.3	Elevation above which <i>dxmin</i> is applied	46
5.4	Number of points per wavelength	49
5.5	Time step	51
5.6	Conclusion	53
6	Single precision	54
6.1	Introduction	54
6.2	Effect of single-precision	54
6.3	Conclusion	54
7	Combined approaches and computation times	55
8	Conclusions and recommendations	59
8.1	Conclusions	59
8.2	Recommendations for BOI	60
9	References	62
A	Sensitivity to random seeding of boundary conditions	64
B	Statistical measures	66
C	Supplementary document with figures	67

1 Introduction

1.1 Background

1.1.1 General

The Dutch dune system is a primary line of defence against coastal inundation and therefore periodic evaluation is required to assure that it fulfils its function. The current assessment of dune safety uses an evaluation method based on the empirical DUROS+ model that was originally developed in the 1980s (Technische Adviescommissie voor de Waterkeringen, 1984; Expertise Netwerk Waterveiligheid, 2007). Currently, limitations in this approach due to underlying assumptions of the empirical model restrict the application of this methodology for large stretches of the Dutch coast (Deltares, 2015). Furthermore, recent research (Deltares/Arcadis, 2019b) has pointed to inaccuracies in DUROS+ for large wave period conditions, thereby reducing the validity of the model for the safety assessment of the Dutch dune coast.

In preparation for the second safety assessment cycle, which starts in 2023, and the *Beoordeling en Ontwerp Instrumentarium* (BOI) project, Deltares and Arcadis developed an Action Plan for the Safety Assessment of Sandy Coasts (“Plan van Aanpak Vernieuwd Instrumentarium Zandige Keringen”, in Dutch; Deltares/Arcadis, 2019a) commissioned by Rijkswaterstaat. The Action Plan for the Safety Assessment of Sandy Coasts, henceforth termed *Action Plan*, describes a transition from the current transect-based safety assessment methodology to an improved, 2DH area-based assessment using the state-of-the-art process-based model XBeach (Roelvink et al., 2009).

To ensure inter-comparability of dune assessment results over multiple assessment cycles, the Action Plan proposes a phased development of the new methodology, with four long-term development phases foreseen. The Action Plan describes a set of tasks to be carried out in development Phase 1 to allow for application of the new methodology in a transect-based approach in the dune safety assessment of 2023. These tasks principally focus on the development and validation of the XBeach model, the development and validation of a probabilistic and semi-probabilistic approach, and a redefinition of the assessment methodology using the new modelling approach.

1.1.2 Current subproject

One of the tasks defined in the Action Plan is to investigate possible approaches to increase the computational efficiency of XBeach simulations. The standard computational time of a two-dimensional (2DH) XBeach model is in the order of a few hours of computation time to simulate one hour of a storm (i.e., the computation time is several times greater than the duration of the storm to be simulated). The standard computation time for a 1D XBeach model is substantially less, being in the order 15 minutes’ computation time per hour of storm simulation. The current task will focus on identifying potential reduction methods to reduce computational time while maintaining acceptable accuracy and consistency in model simulations.

Four approaches to reduce computation time are investigated in this report:

- Make the predictions of the one-dimensional (1D; cross-shore transect-based) XBeach model consistent with the two-dimensional (2DH) area model for alongshore-uniform coasts, by parameterizing the effects of directional spreading in a 1D XBeach approach. This will allow the use of a 1D approach in the safety assessment, instead of a computationally expensive 2DH approach.
- Applying a morphological acceleration factor (*morfac*), which can significantly reduce the computational expense, but also reduces model accuracy and consistency. In this approach the potential reduction in computational time is compared to the model consistency for a range of *morfac* values, in order to derive an optimum *morfac* value.
- Optimizing the temporal and spatial discretization of the model simulation. The number of grid cells needed for an accurate prediction is optimized. Furthermore, the required time step to accurately model the wave transformation and morphological changes is determined. In this approach, guidelines are developed to derive the minimum grid size needed in the dune-area, the maximum grid size needed at the offshore boundary and the maximum acceptable time step.
- Investigating the potential reduction in computational time by modifying the XBeach source code to use single-precision variables instead of the current double-precision variables.

1.2 Research questions

The main research question is: “*What approaches can be applied to reduce computational time in XBeach, without significant loss of consistency in predicted results*”

To answer the main research question, four sub questions are defined:

1. *Can directional spreading be included in a one-dimensional model, in order to be consistent with an alongshore-uniform two-dimensional model?*
2. *How much can a morphological acceleration factor reduce computational time without significant deviations in model accuracy?*
3. *What temporal and spatial discretization can be applied to optimize the computational time without losing model accuracy?*
4. *Will a single-precision approach reduce computational expense?*

1.3 Outline

The general approach will be presented in Chapter 2, together with a brief evaluation of the effect of random wave seeding on the model results. In Chapters 3–6 the four approaches to reduce computational time are tested, and respectively research questions 1–4 are addressed. In a discussion in Chapter 7, the most important reduction approaches are combined and their combined result on the computational time and accuracy are quantified. The report ends with conclusions and recommendations in Chapter 8.

2 Approach

2.1 General approach

To reduce the computation time of XBeach four different potential reduction approaches are considered. For all potential reduction approaches, the reduction in calculation time is placed alongside the impact on the consistency of XBeach model predictions. This consistency is assessed using a set of morphological indicators, which are described in paragraph 2.4. To ensure the analysis is representative for the Dutch coast, model consistency is computed for 26 Dutch coastal profiles (Arcadis, 2020) with corresponding water level and wave conditions applied in the current safety assessment (Paragraph 2.2). To verify the effect of the reduction approach for the desired processes, the 26 representative profiles are forced with both constant and time-varying boundary conditions (Figure 2-1).

In the first approach (Figure 2-1, blue box), the ability of a 1D model with a reduced variance of the short-wave groups, as proposed in Deltares (2020a), to mimic infragravity wave transformations of a 2D model with directional spreading, is studied. For a large range of wave conditions and two schematised profiles, the optimal wave group reduction factor is determined, after which the applied approach is verified for the 26 profiles representing the Dutch coast. These simulations are carried out with constant boundary conditions since this reduction approach is not related to a complete storm development.

A base case of the 26 profiles representing the Dutch coast including the reduction factor for 2D effects from the previous step is defined in Paragraph 2.3. This base contains one uniform set of parameters and model schematizations rules for the 26 profiles. All the other potential reduction topics are compared to this base case of the 26 profiles. In this way it is possible to show the relative improvement or deterioration for each topic with respect to the same base case. In the Chapter 7, the combined effect of all the proposed reduction topics is shown in terms of reduced computational time and model accuracy (including the assumption of a 1D approach).

The second potential reduction approach is the morphological acceleration factor. For the 26 profiles representing the Dutch coast, different values of the morphological acceleration factor are verified for morphological indicators of the 26 representative profiles. Since the morphological acceleration factor affects the time period and thus the storm development, the simulations are computed with constant and varying boundary conditions.

The third potential reduction topic identified is the temporal and spatial discretisation of the model. Similar to the previous reduction approach, the effect of different discretisation methods are studied for the morphological indicators. Both the number of grid cells per wave length, required for accurate wave propagation, and the minimum grid resolution for the dry cells, required for accurate erosion processes, are varied. Furthermore, the timestep expressed in term of the Courant number are varied.

Fourthly, the effects of the floating-point format in the source code is verified. The source code compiled with variables defined with single and double precision are tested for simulations of the 26 profiles with constant boundary conditions.

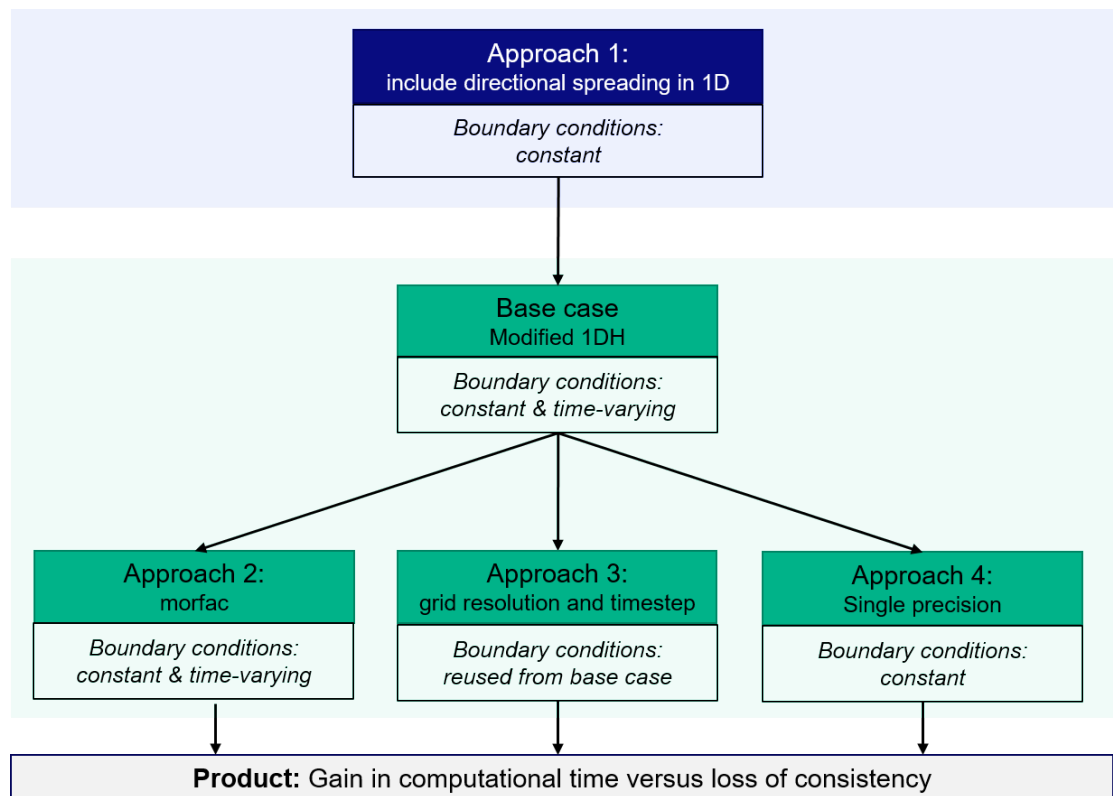


Figure 2-1: Overview of the applied approach to determine the gain in computational time versus the loss in accuracy.

2.2 Input data

2.2.1 Cross-shore profiles

In this study two sets of profiles are used to investigate the reduction in computational time;

- Schematised profiles representative for the Holland coast and a Waddensea profile;
- 26 representative profiles of the Dutch coast based on the measured JARKUS-profiles.

Schematised profiles: Reference profile and Waddensea profile

The schematised profiles used in this study are two profiles that are based on a typical cross-shore profile of the Holland coast and Waddensea coast. These profiles were used in earlier dune erosion research (e.g. WL | Delft Hydraulics, 1982) as well as in the BOI project (Deltares 2020a,b).

The Holland coast profile has a dune top located at NAP +15 m. The slope of the dune face is 1:3 and ends at NAP +3 m. From there on the slope is 1:20 to a level of NAP+0m. From NAP+0m to NAP -3 m the slope is 1:70. From that point on seaward the slope is 1:180, see Figure 2-2. No bars or channels are present on the shoreface. Based on the developed rules for minimum water depth at the offshore boundary in Deltares (2020b), the profile is extended to a depth of -30 m.

The Waddensea profile has a 1/1000 shoreface slope and has been extended to 30 m depth (see Figure 2-3), based on information given in *The Kustgenese 2.0, Atlas of the Dutch Lower Shoreface (Report 1220339 -ZKS – 0068)* and the developed rules for minimum water depth at the offshore boundary in Deltares (2020b).

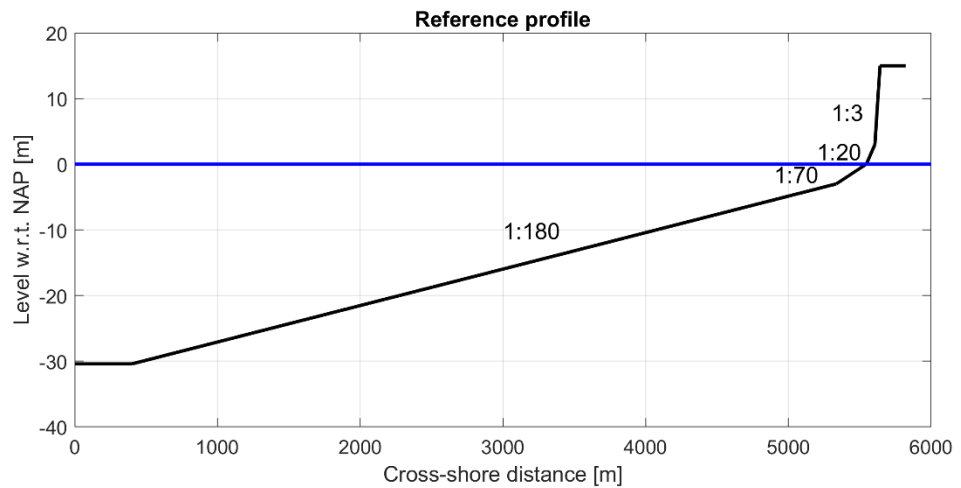


Figure 2-2: Reference profile based on WL | Delft Hydraulics (1982) extended with a 1:180 slope to 30 m.

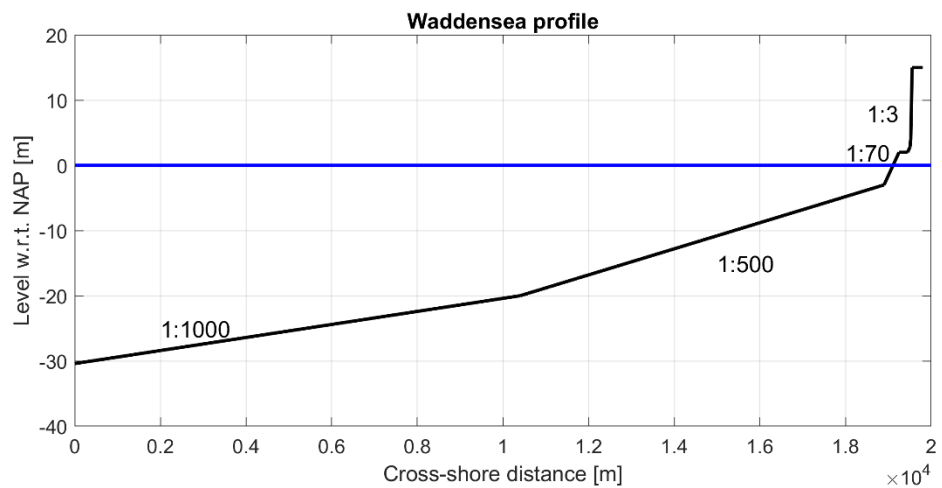


Figure 2-3: Waddensea profile with a 1:1000 slope to a depth of 30 m.

Representative profiles for the sandy Dutch coast

For this project a set of representative profiles of the Dutch coast are derived that can be used for the development of the new methodology in the dune safety assessment of 2023 (Arcadis, 2020). This set includes 26 sandy profiles from the south (Zeeuws-Vlaanderen) to the north (Schiermonnikoog), based on observed (JARKUS) profiles (see Figure 2-4). An overview of the 26 profiles is shown in Figure 2-5 .



Figure 2-4: overview of the location of the selected representative profiles (red lines) (Arcadis, 2020).

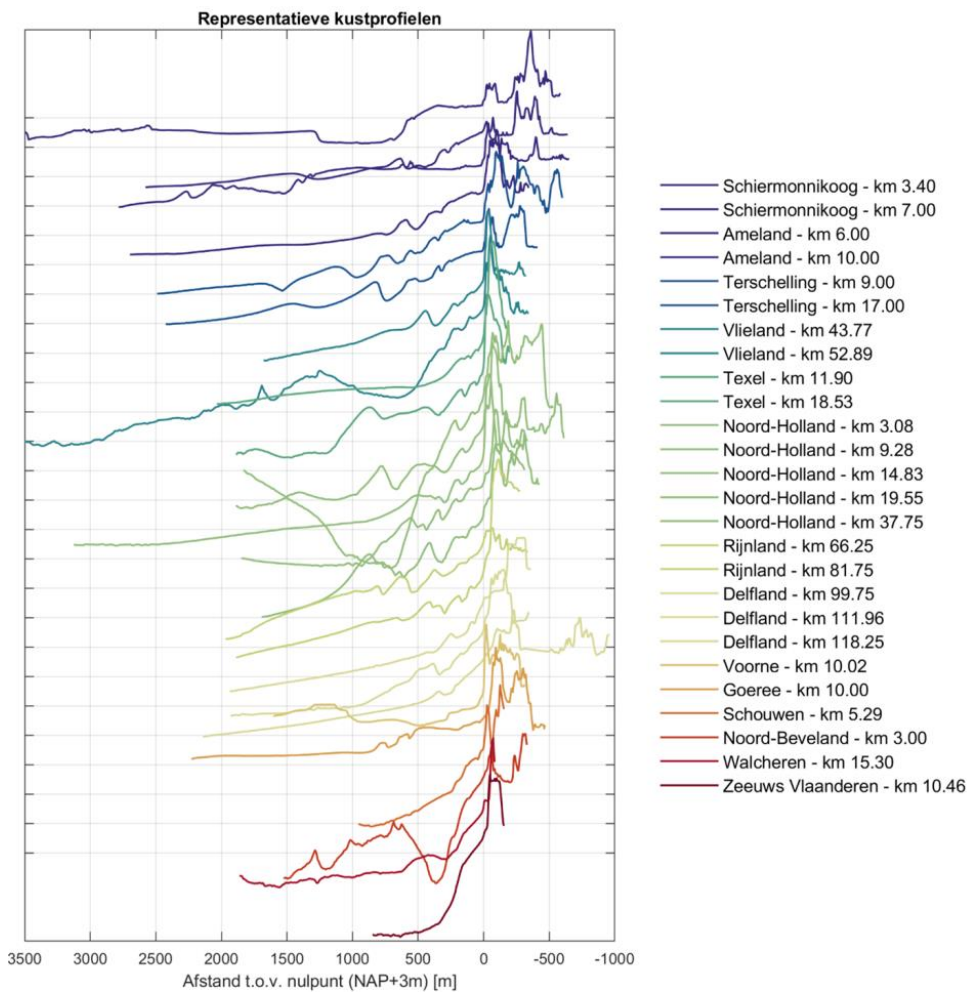


Figure 2-5: The selected representative profiles of the Dutch coast (Arcadis, 2020).

2.2.2 Forcing conditions

In this study both constant and time-varying forcing conditions will be applied, as this could affect the resulting morphological response in the model.

For the time-varying conditions, the approach as derived in Steetzel (1993) is used. The total water level (h) is composed of an astronomical tide and a surge effect, with a shape as shown in Figure 2-6, which is determined from:

$$h(t) = h_0 + h_a \cos \left[\frac{2\pi(t-t_{ma})}{T_a} \right] + h_s \cos^2 \left[\frac{\pi(t-t_{ms})}{T_s} \right] \quad (0.1)$$

Here the first two terms on the right side denote the astronomical effect, with mean water level h_0 (0.45 m) and an M2 tidal component with amplitude h_a of 1.00 m and period T_a of 12.42 hours. The third term represents the surge effect with an amplitude of h_s and a storm duration of $T_s = 45$ h. It is assumed that the maximum astronomical variation coincides with the maximum surge level ($t_{ma} = t_{ms}$). Consequently, the maximum water level equals $h_{\max} = h_0 + h_a + h_s$.

For the time-varying wave conditions, the significant wave height variation $H_s(t)$ and wave period $T_p(t)$ during the standard storm surge is given as:

$$\begin{aligned} H_s(t) &= \hat{H}_s \cos^2 \left[\frac{\pi(t-t_{ms})}{T_H} \right] \\ T_p(t) &= \hat{T}_p \cos \left[\frac{\pi(t-t_{ms})}{T_T} \right] \end{aligned} \quad (0.2)$$

In which the maximum wave height (at time $t = t_{ms}$) is \hat{H}_s and maximum period \hat{T}_p . The duration T_H and T_T are based on the assessment of wave height measurements, and equal 125 h.

The time-varying boundary conditions are applied for a total simulation period of 32 h. The maximum surge height h_s , wave height \hat{H}_s and wave period \hat{T}_p are different for all cross-shore profiles. For the 26 representative profiles these values are based on the hydraulic boundary conditions used in the current dune safety assessment (WBI2017), and are listed for each selected representative profile in Table 2-1. The values are based on the present probability of failure in the signal value (in Dutch “signaleringswaarde”).

Constant forcing conditions are applied for a simulation period of 6 h. The maximum surge height h_s , wave height \hat{H}_s and wave period \hat{T}_p listed in Table 2-1 are used to setup the constant boundary conditions.

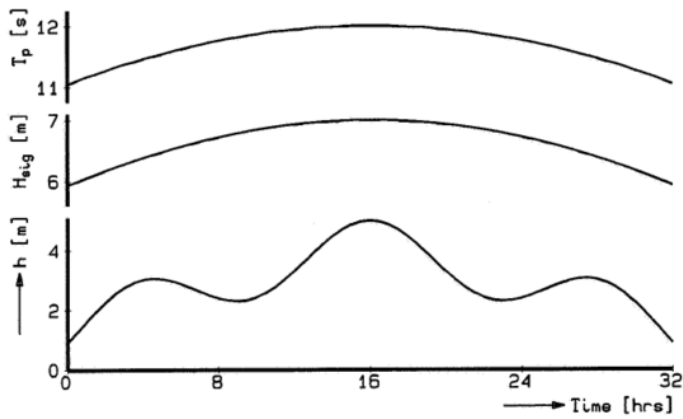


Figure 2-6: Overview of the time-varying hydraulic conditions. Source: Steetzel (1993)

Table 2-1: Overview of hydraulic boundary conditions per representative profile based on the probability of failure in WBI2017 (Arcadis, 2020).

kustvak	Raai [km]	Profile ID	Surge h_s [m + NAP]	\hat{H}_s [m]	\hat{t}_p [s]	D50 [μ m]
Schiermonnikoog	3.40	2000340	4.30	10.15	19.21	166
Schiermonnikoog	7.00	2000700	4.33	10.15	19.46	162
Ameland	6.00	3000600	4.22	10.16	18.68	176
Ameland	10.00	3001000	4.23	10.16	18.77	168
Terschelling	9.00	4000900	4.36	10.74	18.54	158
Terschelling	17.00	4001700	4.39	10.74	18.76	186
Vlieland	43.77	5004377	3.73	9.56	16.65	192
Vlieland	52.89	5005289	3.81	9.53	17.16	191
Texel	11.90	6001190	4.34	10.12	16.96	204
Texel	18.53	6001853	4.28	10.36	17.18	192
Noord-Holland	3.08	7000308	4.41	9.81	16.65	229
Noord-Holland	9.28	7000928	4.45	9.73	16.57	254
Noord-Holland	14.83	7001483	4.51	9.63	16.46	250
Noord-Holland	19.55	7001955	4.55	9.54	16.36	238
Noord-Holland	37.75	7003775	4.8	9.07	15.81	243
Rijnland	66.25	8006625	5.91	9.21	15.76	180
Rijnland	81.75	8008175	5.88	8.82	14.80	218
Delfland	99.75	8009975	5.85	8.45	13.93	209
Delfland	11.96	8001196	5.82	8.05	13.04	211
Delfland	118.25	8011825	5.8	7.83	12.59	251
Voorne	10.02	11001002	5.88	3.10	13.67	150
Goeree	10.00	11001000	5.11	4.04	12.97	207
Schouwen	5.29	13000529	5.18	2.71	12.80	207
Noord-Beveland	3.00	15000300	5.3	3.36	12.40	239
Walcheren	15.30	16001530	5.32	5.09	12.32	308
Zeeuws Vlaanderen	10.46	17001046	5.17	4.40	11.51	204

2.3 Model set-up of the base case

This section describes the model set-up of the base case for the 26 profiles representative for the Dutch coast.

2.3.1 Model grid

For the base case, a model grid is set-up with a high resolution and a small time step to accurately model the wave propagation and morphological changes. This is a conservative model setup, and in Chapter 5 the temporal and spatial discretization of the model setup will be optimized.

A spatially-varying model grid is applied for all profiles, with a higher resolution around the area of interest, i.e. dune face. The grid size on the offshore side depends on the wave length and a required points per wavelength ('ppwl'), while the grid size on the landward boundary is governed by the minimum required grid size 'dxmin'. This minimum required grid size is applied on all cells above a certain reference level (e.g., minimum water level, or maximum storm surge level). Grid sizes in the transition zone between the offshore and landward boundary vary smoothly.

The number of points per wave group is set to 40 points in the base case, using the minimum peak wave period in the forcing conditions to define the wave group length. In addition, the minimum water level during storm conditions is used as the reference level above which the minimum required grid size of 1m is applied. The model grids derived for the time-varying boundary condition simulations are also used for the simulations with constant boundary conditions. Furthermore, all profiles are extended with the criteria for the starting depth as described in Deltares (2020c). An example of such an extended grid is presented in Figure 2-7, in which the different zones are depicted in which 'ppwl' or 'dxmin' are governing for the grid size.

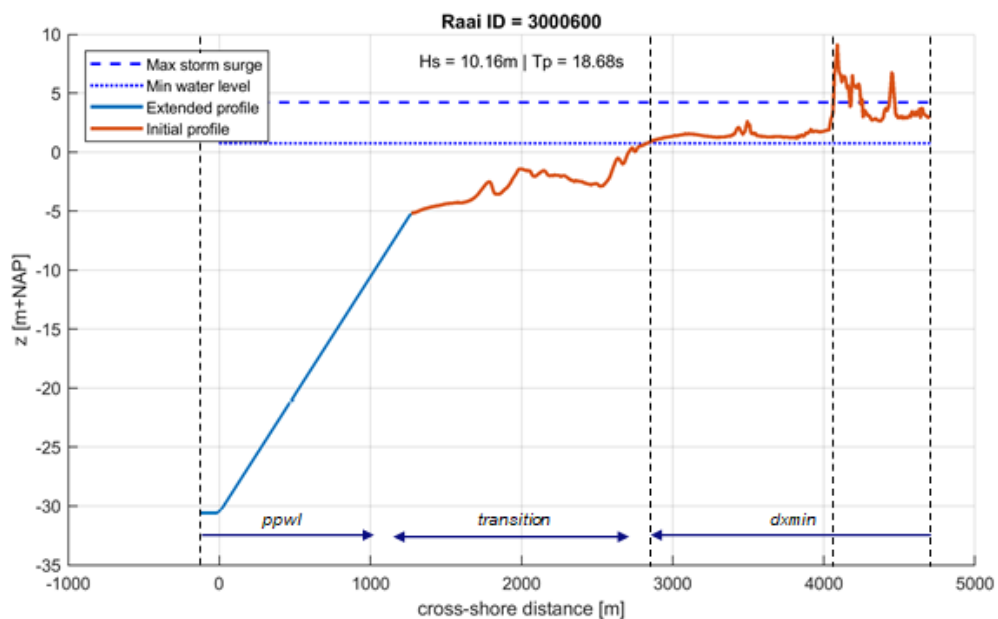


Figure 2-7: Example of a computational grid that is extended to the required starting depth for profileID 3000600. Grid sizes in cross-shore direction are governed by the minimum required points per wavelength (ppwl) near the offshore boundary and by the minimum required grid size (dxmin) near the landward boundary.

To determine the correction for the effects of directional spreading (modified 1D approach), 2D simulations are applied as reference simulation. These 2DH models have the same model settings and bathymetry as the 1D model except for the alongshore-uniform extension of the

grid in the 2DH model. The required alongshore length and alongshore grid resolution is based on the alongshore length scale given the forcing wave conditions (Deltares, 2020a). The grid resolution is given by the alongshore length scale divided by 20 with a minimum of 20 m. The alongshore length of the model is given by two times the alongshore length scale.

2.3.2 Model settings

The BOI model parameter values as derived in Deltares (2020b) are applied in all the computations (Table 2-2. For all the other parameters, except those described in this section, default values are applied). The morphological update of the bed level starts after 1200 seconds to prevent that the initial waves affecting the morphology (*morstart* = 1200). For the initial 1200s of the simulation period, forcing conditions as defined on *t* = 0 (Figure 2-6) are used. In the case of a constant water level, *epsi* is set 0 zero to prevent that artificial wave affects the results (*epsi* is not necessary since there is no water level variation). When a time-varying water level is applied, the *epsi* parameter is set to -1 with *tidetype* set to *hybrid*. The parameter *nufac* is set 0 to prevent that the turbulence model affect the results when the grid resolution is varied. To reduce the computational time of the two-dimensional models, the *single_dir* option is disabled and the wave direction is computed with Snell's law (*snells* = 1). This is a valid assumption for offshore wave directions perpendicular to the coast line in an alongshore-uniform environment.

In the upcoming chapters, the variations in the *morfac* and *CFL* parameters are verified. In the base case these two parameters are set to the default value which is 0.7 for the *CFL* condition and 1 for the *morfac* parameter.

Table 2-2: Overview of BOI model parameters applied in the simulations.

Parameter	Value
Bedfriction (BOI parameter)	mannings
Bedfriccoef (BOI parameter)	0.02
Waveform (BOI parameter)	Vanthiel
facSk (BOI parameter)	0.13
facAs (BOI parameter)	0.10
Break (BOI parameter)	Roelvink_daly
Gamma (BOI parameter)	0.51
Gamma2 (BOI parameter)	0.31
Alpha (BOI parameter)	1.37
Beta (BOI parameter)	0.11
Wetslp (BOI parameter)	0.25
morstart	1200
Deltahmin (BOI parameter)	0.1
Fixedavalttime (BOI parameter)	0
oldTsmmin (BOI parameter)	0
Oldhmin (BOI parameter)	0
epsi	0 (constant water level); -1 (time varying water level)
Tidetype (only with a time varying water level)	hybrid
nufac	0
Single_dir (only 2DH simulations)	0
Snells (only 2DH simulations)	1

2.4 Morphological indicators

The primary focus within the project is to be able to predict morphological change during storm conditions using the XBeach model. Three indicators were defined in Deltares (2020b) for the assessment of these morphological predictions: dune erosion volume, dune retreat and foreshore slope. Since the new assessment methodology will be defined in terms of erosion volume (Rijkswaterstaat, 2020), the dune erosion volume is the most important of the three indicators.

The dune erosion volume is defined as the difference in volume above a vertical datum per meter alongshore between the initial bed level and the bed level at a given time. The maximum still water level is applied as lower vertical datum for this computation, see Figure 2-8a. The dune front retreat is the landward migration of the dune front. It is defined as the horizontal displacement at a given reference height in the considered time period. The reference height is defined as 1.5 times the grid resolution below the maximum initial bed level (see Figure 2-8b). This height is representative for the dune front and low enough to capture all the dune front of all the observed profiles. The dune height can reduce during an experiment due to erosion. The foreshore slope is defined as the mean slope in the deposition zone. The upper limit is defined as the maximum water level, and the lower limit is equal to the most seaward point of the deposition zone, where the deposition is equal to 50% of the maximum vertical deposition (see Figure 2-8c). The mean of this slope is computed after interpolating the bed level to a uniform grid. This interpolation is required to prevent that the mean berm slope is affected by the spatial variation in the grid.

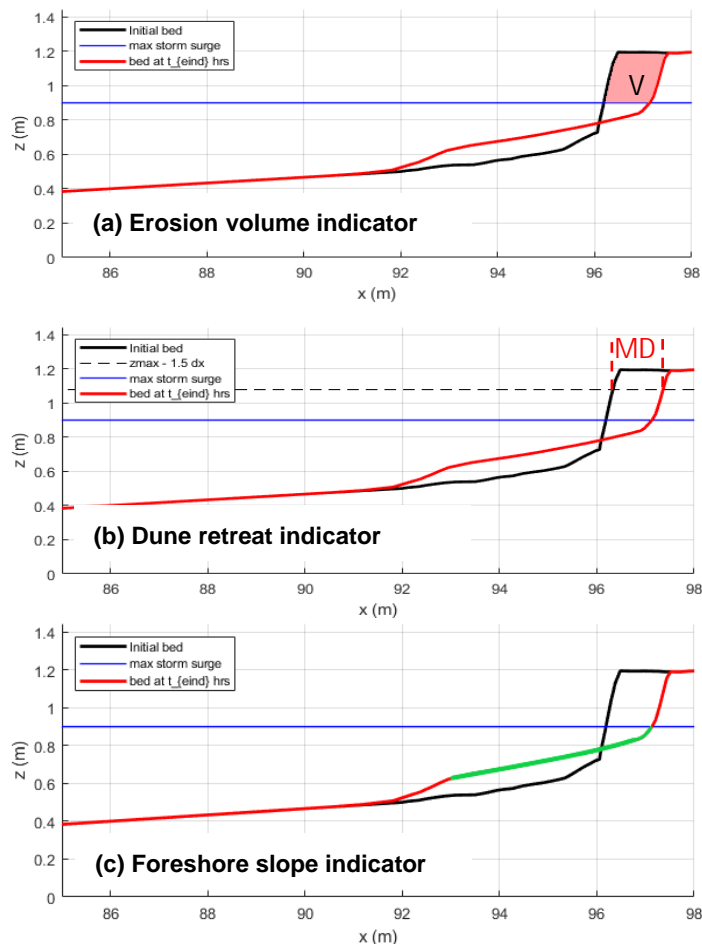


Figure 2-8: Schematic overview of the three morphodynamic indicators; erosion volume (a), dune retreat (b) and foreshore slope (c).

2.5 Evaluation measures

To determine the gain and loss of the applied reduction approaches, the statistics of the speed-up factor and the erosion volumes over the 26 profiles are computed. For every reduction approach the mean and standard deviation of the speed-up factors are computed with the following definition of the speed-up factor,

$$\text{speed-up factor} = \frac{\Delta t_0}{\Delta t_r} \quad (0.3)$$

where Δt_0 is the simulation time of the base case and Δt_r the simulation time of the applied reduction approach. In a similar way, the ratio of the erosion volumes is computed,

$$\text{Ratio erosion volume} = \frac{V_r}{V_0} \quad (0.4)$$

where V_0 is the erosion volume of the base case and V_r the erosion volume of the reduction approach. Besides the mean and standard deviation, the spread over the 26, 22 and 18 profiles with the lowest error are shown. The spread over 26 profiles represents the entire range in relative erosion volumes (maximum-minimum relative erosion volume). The spread over 22 profiles then excludes two profiles with the largest and two profiles with the smallest relative erosion volume ratios, hence the most sensitive profiles are excluded. Likewise, the spread over 18 profiles excludes the four profiles with the largest relative erosion volume and the four profiles with the smallest relative erosion volumes. Therefore, these spreads are used to get a feeling whether certain measures affect all profiles, or that only specific profiles turn out to be sensitivity to that measure.

2.6 Effect of random wave seeding on dune erosion volumes

In the XBeach model, two different boundary conditions are needed at the boundary, namely a time-varying wave group signal of the short-wave energy and the corresponding incoming infragravity wave signal. Both time series are generated internally by the XBeach model based on a random wave field related to a user-defined input wave spectrum. The wave group signal is given by the envelope of this random wave field. This means that there is a variation in the morphodynamic predictions by XBeach due to the randomness of the wave train seeding. To quantify the effect of this random seeding, the dune erosion volumes are computed for 100 different simulations with the same wave conditions, but different wave trains. The ten simulations are run for both reference profiles with constant tidal and wave conditions for a period of 6 h, as well as with varying tidal and wave conditions for a period of 32 hours.

In Appendix A, the resulting mean, minimum, maximum, 10th and 90th percentile of the calculated dune erosion volumes (based on the 100 runs) are listed for the two reference profiles and two types of boundary conditions (steady and time varying). In addition, the relative deviations in dune erosion volume with respect to the mean are listed. In general, random wave seeding results in approximately 2–3 % deviation in erosion volumes. To exclude this effect from the results of simulations where possible accelerations are assessed, the exact boundary conditions time series of the base case simulations are reused where possible. However, where this is not possible (e.g., while using morfac or single precision), the wave seeding effect should be included in the interpretation of the results.

3 Including the effects of directional spreading in a 1D XBeach approach

3.1 Introduction

The infragravity wave response of a one-dimensional model (1D, without directional spreading) is significantly different from that of a two-dimensional model (2DH) including directional spreading (Klopman and Dingemans, 2001). The infragravity wave height is significantly lower in a wave field with directional spreading in which the waves interact less to produce infragravity waves, than a wave field with all waves propagating in the same direction (as for example in a wave flume, or a 1D XBeach model), in which all waves fully interact. Note that this is not a model artefact, but a natural phenomenon.

XBeach is capable of generating boundary conditions for wave fields with and without directional spreading. In a 2DH model (including directional spreading), the wave-groups vary both in cross-shore and alongshore direction, which means that the radiation stresses, forcing the infragravity waves, also vary in both directions. However, in a 1D model the variation in alongshore direction does not exist and, therefore, all energy transfer from the wave groups to the infragravity waves occurs in the cross-shore direction. This results in a higher infragravity wave height in the 1D model domain as compared to a 2DH model.

While thus more representative of the natural processes, a 2DH model requires much computational time, which may hamper application in the dune safety assessment. Therefore, an adjusted short wave-group signal at the boundary of the 1D model was proposed in Deltares (2020a) to compensate for the absence of directional spreading effects. It was shown that by means of an α_E parameter, which reduces the short wave-group variance at the boundary the reducing effects of directional spreading could be mimicked in a 1D model.

In this chapter we investigate whether it is possible to correctly model the infragravity wave transformation in a 1D model with this α_E parameter for a large range of conditions applicable for the Dutch coast. First, the α_E parameter is calibrated for a range of wave conditions for the Reference and Waddensea profile, after which the obtained α_E parameter is validated for 26 representative profiles of the Dutch coast.

3.2 Implementation

Infragravity wave growth in the XBeach model is controlled by radiation stress (wave) forcing terms in the non-linear shallow water equations solved in the XBeach flow module. As such, there is no simple source or sink infragravity energy balance term available to tune in a modified 1D approach. Instead, infragravity wave heights can either be modified by dissipating infragravity waves more strongly (i.e., through increased viscosity or bed roughness), or by reducing the mechanisms for infragravity wave growth. Of these two options, increased dissipation through higher viscosity or bed roughness has the drawback of slowing flow in general, leading to increased predictions of wave set-up at the coast, in addition to this solution being nonphysical. Therefore, reducing the mechanisms for infragravity wave growth is preferred as it is an approximation of the natural process of reduced forcing in a directionally-spread wave field.

We hypothesize that the infragravity wave height will reduce when the variation (in time and space) of the wave group height is reduced, while maintaining the same time-averaged wave height. In this way, time- and spatially-varying radiation stress gradients are reduced, leading to less energy transfer to the infragravity waves, and hence smaller, more realistic infragravity waves. If the mean wave height remains unchanged, the model will still accurately predict mean current circulation and setup. To verify this behavior, the time-varying wave group signal at the boundary is adjusted by a reduction factor (α_E). The boundary signal of the wave groups is now given by:

$$E_{new}(t) = \alpha_E (E_{old}(t) - \langle E_{old}(t) \rangle) + \langle E_{old}(t) \rangle \quad (0.5)$$

Where E_{old} is the computed short-wave energy time series at the boundary and $\langle \dots \rangle$ represents the averaging operator over the entire time series. When the reduction factor α_E is set to 1, the imposed wave group time series is identical to a regular wave group signal for a 1D model. When the factor is smaller than 1, the variance of the wave group signal in time is reduced (Figure 3-1). Note that the mean of signal is unchanged, which means that the mean short-wave height at the boundary is unaltered.

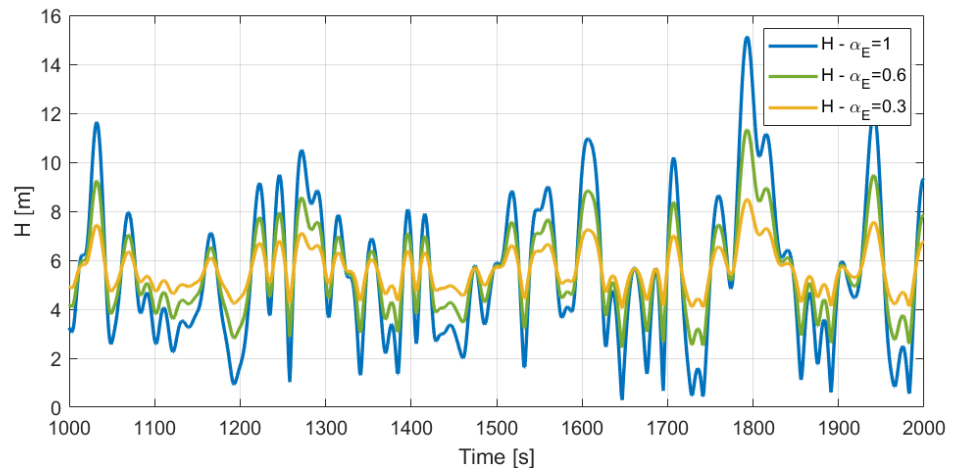


Figure 3-1: Time series of the instantaneous wave height for three different α_E values.

3.3 Calibration

This section describes the calibration of the α_E parameter for a range of wave conditions and two profiles. First the model setup is described, followed by the results of these simulations. Thereafter, the optimal α_E parameter is presented with the corresponding improvement for the different indicators.

3.3.1 Setup

To calibrate the α_E parameter, a 1D model with variations in α_E is compared to an alongshore-uniform 2DH model for a range of wave conditions and two different profiles (Table 3-1). The variations in wave conditions are representative for the Dutch coast and vary from a 5 m wave height with a period of 11 s to a more extreme wave height of 9 m with long wave periods of 20 s (Deltares, 2016). Currently, the directional spreading is not specified in the hydraulic boundary conditions, but 30° is a representative value for a storm on the North Sea. To study the effects of variations in the directional spreading, a directional spreading of 10° , 15° , 30° and 50° is tested. To check whether the α_E parameter is sensitive for the profile-shape, the simulations are computed for two different profiles: the Reference profile and the Waddenzee profile. The reference profile is relatively steep, whereas the foreshore slope of the Waddenzee

profile is relatively gentle with a bank at the foreshore. A surge level of 5 meter is applied in all the simulations to model realistic storm conditions.

All combinations of wave height, peak period, directional spreading, profiles and α_E as listed in Table 3-1 are tested, resulting in $3 \times 5 \times 4 \times 2 \times 7 = 840$ simulations in total.

Table 3-1: Variations applied in the calibration of the α_E parameter.

Parameter	Applied variation	Applied in 1D and/or 2DH
Wave height [m]	5, 7 and 9	1D and 2DH
Peak period [s]	8, 11, 14, 17 and 20	1D and 2DH
Directional spreading [°]	10, 15, 30 and 50	1D and 2DH
Profile	Reference profile and Waddenzee profile	1D and 2DH
α_E [-]	0.2, 0.3, 0.4, 0.5, 0.6, 0.8 and 1.0	1D

For each simulation, the nearshore infragravity wave height at a depth of 5 m, the erosion volume above mean sea level, the dune retreat and the foreshore slope (see Figure 2-8) are computed. In the 2D simulations these indicators are averaged over the 20 most central transects in the domain. The infragravity wave height is computed as,

$$H_{m0,LF} = 4\sqrt{m_0} \quad (0.6)$$

where m_0 is the variance of the water level.

3.3.2 Results

The effects of the α_E parameter on the modelled wave height and profile development is shown using an example simulation in Figure 3-2, and it represents the reference profile with an offshore wave height of 7 m, peak period of 20 s and directional spreading of 30°. The 1D simulations without a reduction of the variance in the short-wave group signal ($\alpha_E = 1$) shows a large overestimation of the infragravity wave height compared to the alongshore-uniform 2DH model (Figure 3-2, B). The nearshore infragravity wave height is approximately 5 m for a 1D model, whereas the 2DH model results in a nearshore infragravity wave height of 2 m. In this case an α_E of 0.3 would most closely resemble the 2DH infragravity wave height transformation.

A consequence of the reduction approach is that the short-wave transformation is slightly different to the 2DH model (or 1D model with $\alpha_E=1$). An α_E smaller than 1 reduces the short-wave group signal variance, which leads to a smaller breaker zone as the short-waves break closer to each other. Therefore, the short-wave height in the breaker zone shows a less gradual spatial distribution for an decreasing α_E (Figure 3-2, A). This effect is particularly visible for simulations with $\alpha_E = 0$. However, these changes to the breaking zone do not have an significant effect on the dune erosion (Figure 3-2, C) since the short-wave height close to the shoreline is similar for all values of α_E (Figure 3-2, A).

The variation in infragravity wave height for different values of α_E has an effect on profile development (panel C of Figure 3-2). Compared to the 2DH simulation, the 1D model without reduction overestimates the dune erosion volume (approximately 20%). If an α_E of 0.3 is applied, the erosion profile matches with the 2DH erosion profile.

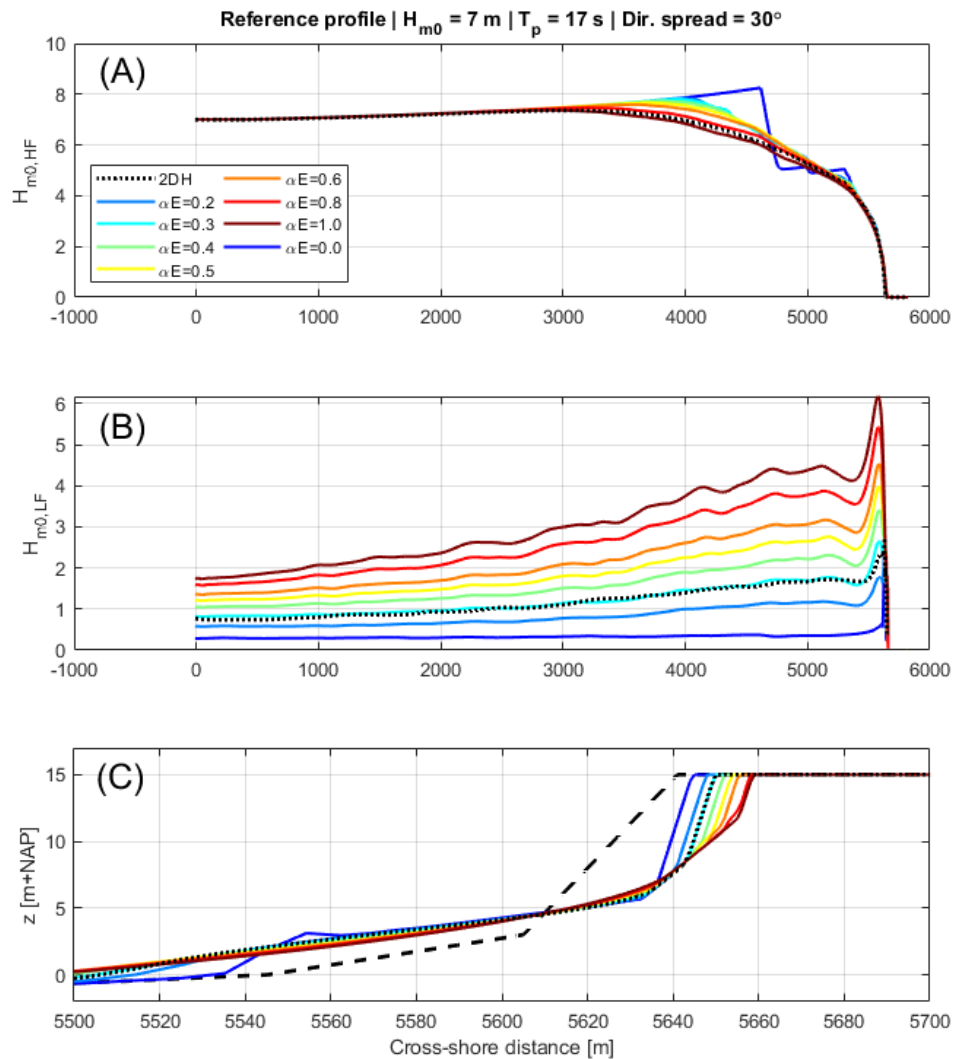


Figure 3-2: Effect of the α_E value on the short wave height (panel A), infragravity wave height (panel B) and erosion profile (panel C). The colours indicate the 1D results with variations of the α_E parameter. The solid black line shows the 2D result. In the lower panel the initial profile is shown with a dashed black line.

The sensitivity of the morphological indicators (erosion volume, dune retreat and foreshore slope) and the infragravity wave height to variations in α_E are shown in Figure 3-3, based on the results shown in Figure 3-2, and are compared to the 2DH results (black line in Figure 3-3). The infragravity wave height, dune erosion volume and dune retreat show a similar trend. For this particular combination of simulations an optimum value for the $\alpha_E \approx 0.3$ can be derived (Figure 2-3 panel A, B and C). The foreshore slope does not show a clear trend with the α_E parameter. Note that the variation in the foreshore slope is very small.

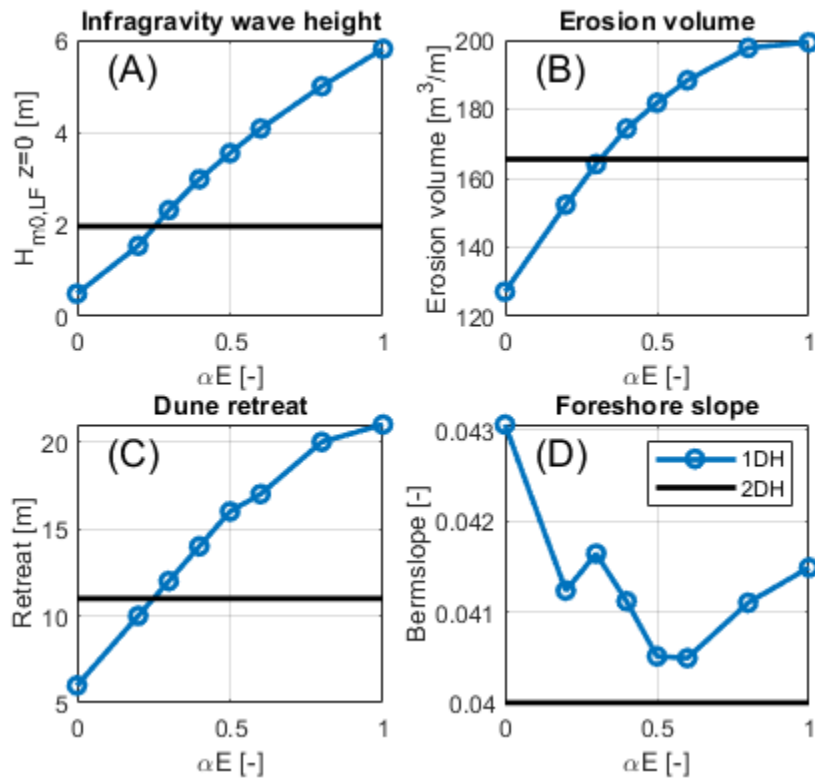


Figure 3-3: Trends of the infragravity wave height at a depth of 5 m (panel A), the erosion volume above still water level (panel B), the dune retreat (panel C) and the foreshore slope (panel D) as a function of the α_E . The solid black line shows the 2D results. These trends correspond to the simulation of an offshore wave height of 7 m with peak period of 17 s and 30° directional spreading for the Reference profile.

Before an optimal α_E parameter can be selected, the optimal α_E parameter for each combination of the wave period, wave height and directional spreading is investigated. The method shown in Figure 3-3 is used to derive an optimum α_E parameter for each combination of forcing conditions. Figure 3-3 The 1D results are plotted as a function of the α_E parameter and compared to the 2DH results, the intersection provides the optimum α_E parameter. When there is no intersection the nearest point is selected as optimum.

For both the Reference profile (Figure 3-4) and the Waddensea profile (Figure 3-5), the sensitivity of the optimal α_E parameter to the forcing conditions is shown. The majority of the conditions require an α_E ranging between 0 and 0.6 to obtain similar results as in the 2DH model (Figure 3-4 and Figure 3-5) for the nearshore infragravity wave height and dune erosion volumes. The optimum α_E parameter is not shown for the foreshore slope and the dune retreat indicators, as the foreshore slope contains a lot of scatter and the dune retreat does not always result in an optimum (e.g., all α_E variations results in the same dune retreat value).

The wave conditions with a directional spreading more than 15° show an optimum α_E parameter of approximately 0.3, and do not display a dependency to the other wave conditions (panels A to D in Figure 3-4 and Figure 3-5). The wave conditions with directional spreading under 15° are more sensitive to the peak wave period T_p (Figure 3-4, panel E, F, G and H). Moreover, the offshore wave height also affects the optimal α_E parameter, for increasing wave heights a lower α_E parameter is required. These trends are similar for the nearshore infragravity wave height and dune erosion volumes.

For the Waddensea profile the trends in dune erosion volumes and the nearshore infragravity wave height differentiate in some cases (Figure 3-5). One reason for this deviation is that different shapes in the post-storm profiles can still result in a similar erosion volume as predicted by the 2DH model. Furthermore, the erosion volumes of the Waddensea profile are generally much lower than the reference profile, which results in more scatter in the relative difference of erosion volumes for the Waddensea profile.

The differences between the two profiles are however not large. Both profiles show a similar behaviour of the α_E parameter as function of the wave conditions (Figure 3-4 and Figure 3-5). This indicates that the optimal α_E parameter is not affected by the profile and that one optimal α_E parameter may be derived for different profile shapes.

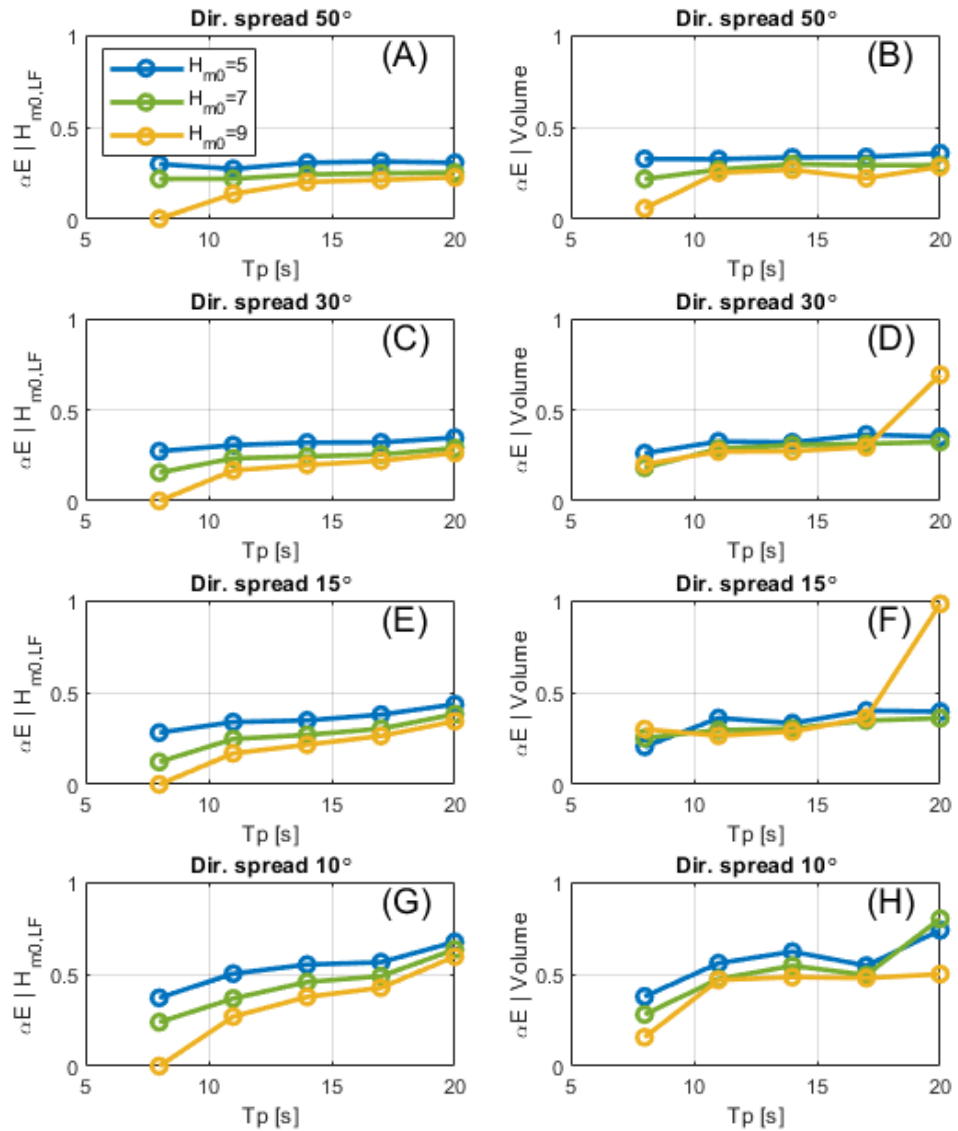


Figure 3-4: Optimal α_E parameter for the nearshore infragravity wave height (left panels) and dune erosion volume (right panels) at the reference profile. The α_E parameter is shown as function of the peak period in each subplot with the variation of the wave heights shown with different lines. The variation in directional spreading are shown in the different subplots.

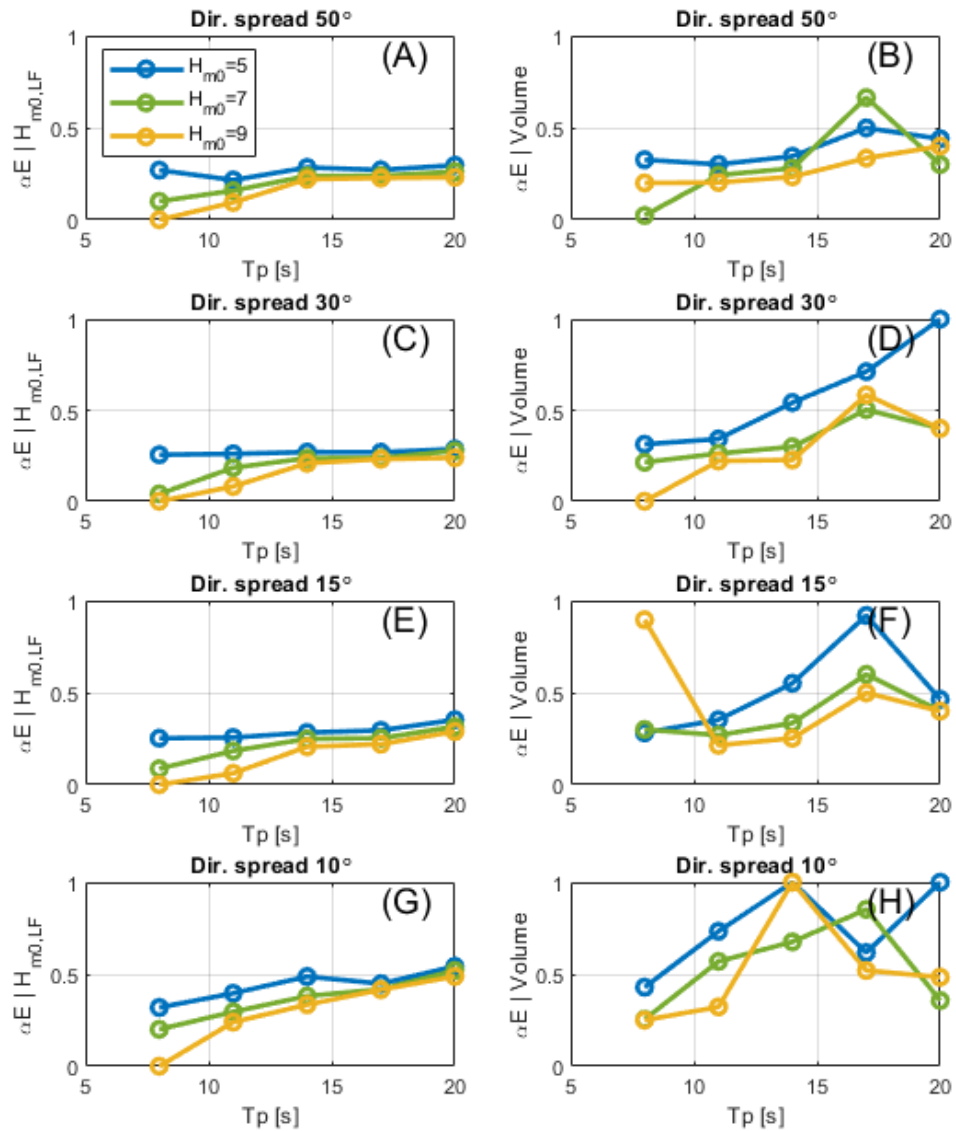


Figure 3-5: Optimal α_E parameter for the nearshore infragravity wave height (left panels) and dune erosion volume (right panels) at the *Waddensea* profile. The α_E parameter is shown as function of the peak period in each subplot with the variation of the wave heights shown with different lines. The variation in directional spreading are shown in the different subplots.

3.3.3 Optimal alpha-E

To determine the optimal α_E parameter, two different regimes are identified. A single α_E parameter can be applied for the wave conditions with a directional spreading of 30–50° degrees (see Figure 3-4 and Figure 3-5). For wave conditions with less directional spreading, it appears that the optimal α_E parameter differs for variations in the peak period. Since these conditions with little directional spreading (i.e. swell waves generated far away without wind waves) are less relevant for storm conditions along the Dutch coast, a separate optimal α_E parameter is derived for these conditions.

Directional spreading of 30° and higher

For the directional spreading of 30–50° the correlation coefficient (R^2) between all the 2DH results and 1D results for variations in α_E is computed. The maximum correlation coefficient is found for a **α_E parameter of 0.3**, considering the nearshore infragravity wave height, dune erosion volumes and the dune retreat for the two profiles (Figure 3-6).

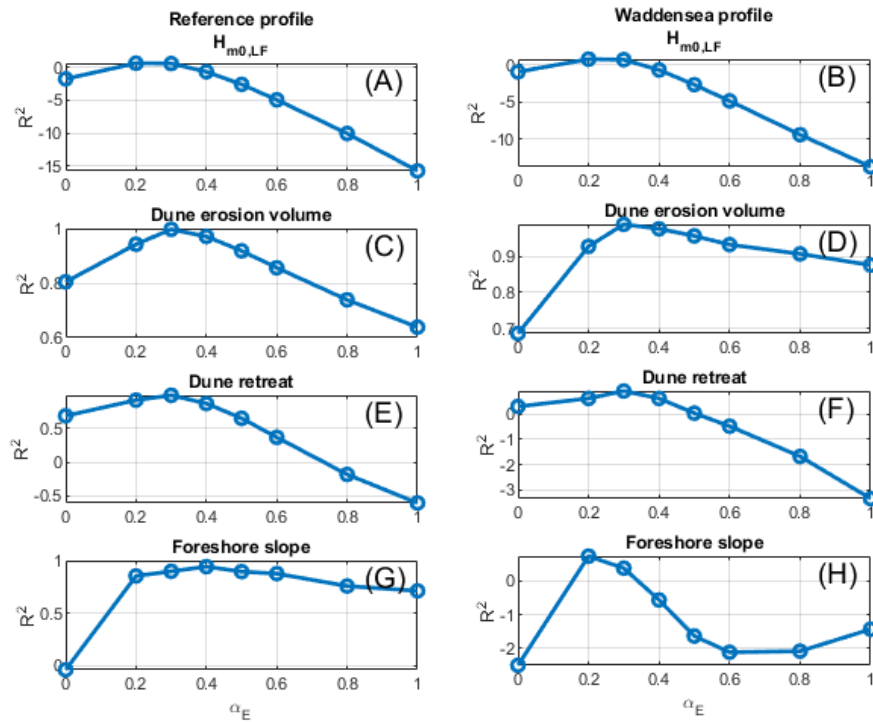


Figure 3-6: Correlation coefficient R^2 as function of the α_E parameter for the nearshore infragravity wave height (panel A and B), dune erosion volume (panel C and D), dune retreat (panel E and F) and foreshore slope (panel G and H). The results for the reference profile are shown in the left panel and the right panel shows the results for the Waddensea profile.

Application of an α_E parameter of 0.3 for the cases with a directional spreading of 30° or 50° results in a significant improvement in the nearshore infragravity wave height compared to no reduction in wave-group variance (Figure 3-7A and Table 3-2). This also leads to a dune erosion volume (Figure 3-7B) and dune retreat (Figure 3-7C) that is more consistent with the 2DH results. The scatter in the dune erosion volumes (SCI = 0.0245) is lower than in the 1D model without short-wave group reduction (SCI = 0.2223). Moreover, the improvement in the dune retreat (Figure 3-7C) also indicates that the post-storm profile is better captured by applying an α_E parameter of 0.3.

Table 3-2: Statistical scores for the comparison of the 1DH model results with the 2DH model results. The definition of the relative bias and scatter index is given in Appendix B. The statistical scores are computed over all wave conditions and profiles with a directional spreading of 30° and 50°.

Indicator	Modified 1D		1D	
	Rel. bias [-]	SCI [-]	Rel. bias [-]	SCI [-]
Nearshore infragravity wave height	0.22	0.29	1.73	1.99
Dune erosion volume	0.0012	0.0245	0.1593	0.2223
Dune retreat	0.0313	0.1482	0.9727	1.2611
Foreshore slope	0.0405	0.0643	0.2223	0.1210

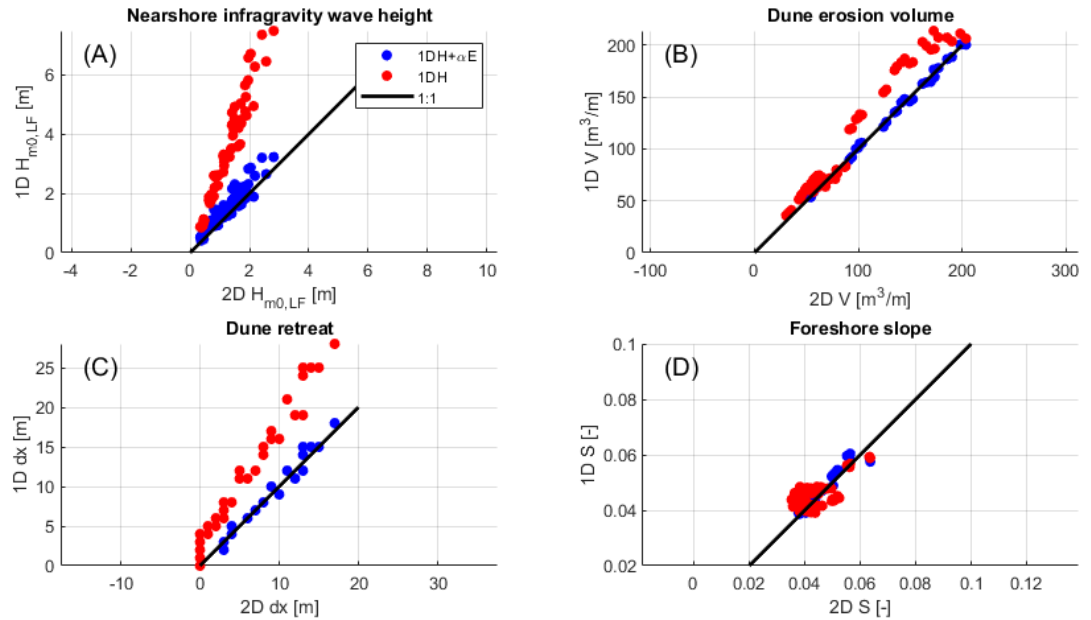


Figure 3-7: Scatter plot of results from 2DH simulation compared to the result of a 1DH simulation for the nearshore infragravity wave height (panel A), erosion volume (panel B), dune retreat (panel C) and foreshore shore slope (panel D). The red dots indicate the result of a simulation with an α_E of 1 and the blue dots the result with an α_E of 0.3 for all the simulations with a directional spreading of 30° and 50° degrees for both the Reference and the Waddensea profile.

Directional spreading lower than 30°

A different α_E parameter is derived for the simulations with a directional spreading lower than 30° degrees, which correspond to more swell-like conditions. For these simulations, the optimal α_E parameter is more sensitive to variations in the peak period and the directional spreading.

The overall sensitivity of the optimal α_E parameter to peak period and directional spreading is captured by calculating the mean optimal α_E , i.e. the optimal α_E averaged over the two profiles and wave heights for the nearshore infragravity. This mean optimal α_E is shown in Figure 3-8 as function of the directional spreading and the peak period. It shows that optimal α_E parameter increases for a larger wave period up to a α_E parameter of 0.6 ($T_p = 20$ s and dir. spread = 10°). This means that sea states without much directional spreading would require a higher α_E parameter (less reduction of short-wave group variance) for an increasing peak period. However, these conditions are not thought likely to occur during periods of large surge at the Dutch coast as these conditions represent swell waves generated by storms far away from the coast. For cases with a directional spreading of more than 30° (right to the red dotted line in Figure 3-8), an α_E of 0.3 is sufficient and is not affected by variations in T_p .

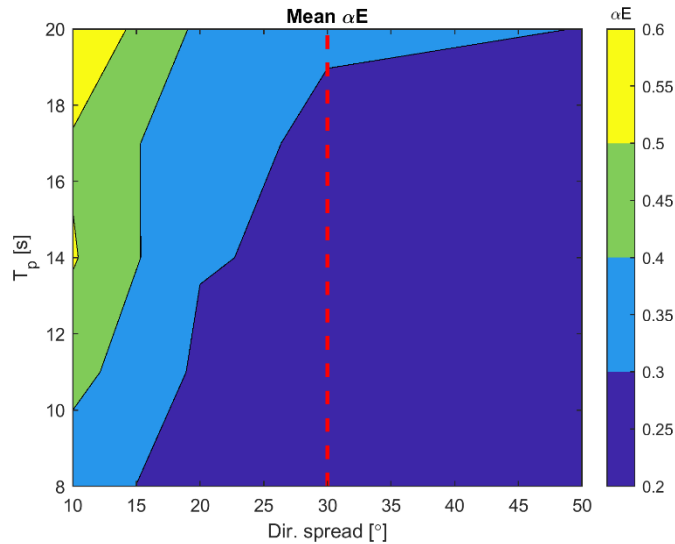


Figure 3-8: Mean optimal α_E parameter over different wave heights and the two profiles for a combination of directional spreading and peak periods. The optimal α_E parameter is derived based on the nearshore infragravity wave height. The red dashed line indicates the directional spreading of 30°.

3.4 Validation

The calibrated α_E parameter of 0.3 is applied for the 26 profiles representative for the Dutch coast, see chapter 2.2. For every profile, the 1D results with an α_E of 0.3 (the 'modified 1D') is compared to the 2DH results with a directional spreading of 30°. For the completeness the 1D with an α_E parameter of 1.0 (no reduction) is also computed.

As an example of the effect of the modified 1D approach on the results of individual profiles, results for two representative profiles are presented in more detail. The first profile is representative for the coast south of the Hondsbossche Zeewering (Figure 3-9). The simulation including the α_E approach shows a different short-wave transformation in the offshore region, where the waves start to break closer to the shore (Figure 3-9A). However, the nearshore short-wave height computed landward of $x = 2000$ m is similar to the 2DH model. The α_E approach leads to infragravity wave transformation (Figure 3-9B) and dune erosion profiles (Figure 3-9C) that are consistent with the 2DH model. The 1D model without the α_E reduction leads to a large overestimation of the infragravity wave height compared to the 2DH model, as well as substantially higher retreat of the dune and a milder-sloped erosion profile.

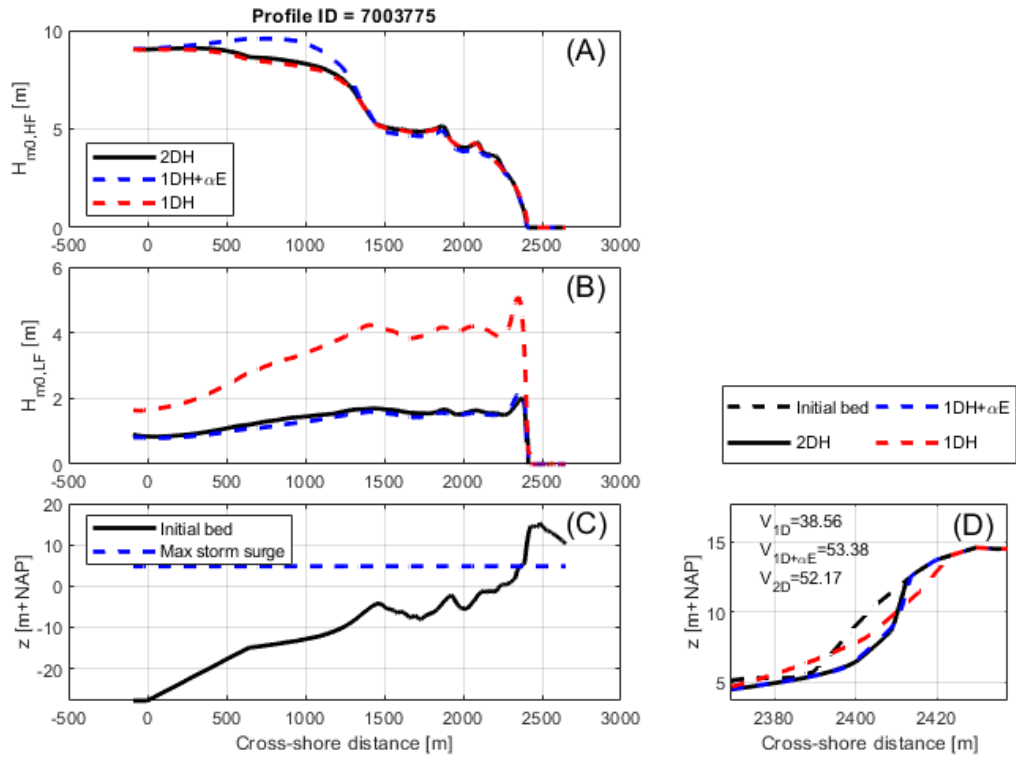


Figure 3-9: Short-wave transformation (panel A), infragravity transformation (panel B) and bed level (panel C) for profile 7003775. In panel D a zoomed region of the erosion profile is shown. The black lines show the results for a 2DH model and the dashed blue line represents the 1D model with a α_E of 0.3. The dashed red line shows the results with 1D model without an α_E reduction.

The second profile is representative for Noord-Beveland and shown in Figure 3-10. This profile is selected because the deviation with the 1D+ α_E approach compared to the 2DH results is relatively large due to overwash in the 1D model. Similar to the previous case, the 1D model without α_E reduction overestimates the infragravity wave, but now results in large amounts of overwash as a consequence. Reducing the short-wave group variance with the α_E parameter results in an infragravity wave height that is more consistent with the 2DH simulation, but now with a small underestimation of the infragravity wave height. Due to the lower infragravity wave height, the dune erosion is lower than for the 2DH result, but is still a significant improvement compared to the 1D result without the α_E approach.

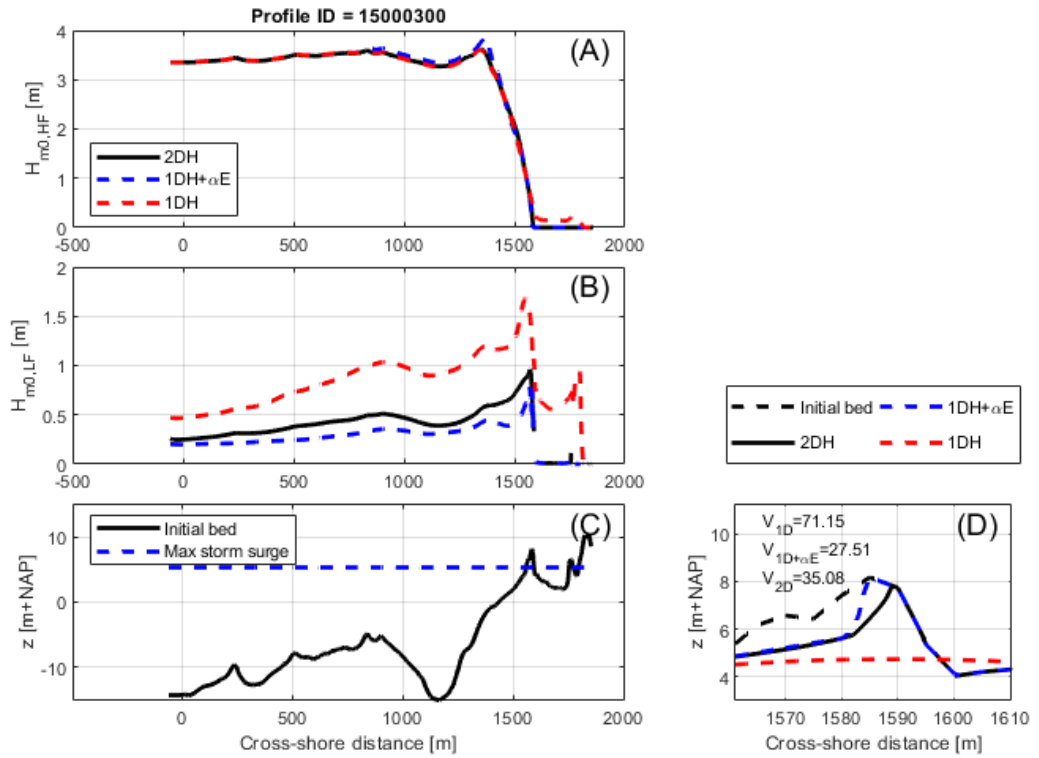


Figure 3-10: Short-wave transformation (panel A), infragravity transformation (panel B) and bed level (panel C) for profile 15000300. In panel D a zoomed region of the erosion profile is shown. The black lines show the results for a 2DH model and the blue dashed line represents the 1DH model with a α_E of 0.3. The dashed red line shows the results with 1DH model without an α_E reduction.

The results of all 26 representative profiles are presented as scatterplots in Figure 3-11, comparing the 1D and modified 1D approach to the 2DH results for the infragravity wave height and all morphological indicators (dune erosion, dune retreat and foreshore slope). The modified 1D approach with an α_E of 0.3 results in a significant improvement of the nearshore infragravity wave heights for all 26 profiles (blue dots in Figure 3-11, panel A). This reduction in the infragravity wave height is similar as found in the calibration but contain more scatter due to the complex bathymetry of some of the profiles. For the dune erosion volumes the modified 1D approach (blue dots in Figure 3-11, panel B) is more consistent with 2DH compared to 1D without reduction in the wave-group signal (red dots in Figure 3-11, panel B), mainly due to improving the more extreme dune erosion cases caused by overestimating the infragravity wave heights (as shown in Figure 3-10). The large overestimation of the infragravity wave height in the 1D model is not seen in the dune erosion volumes (comparing red dots in panel A and B in Figure 3-11), but this trend is visible in the dune retreat. This means that for some conditions in the erosion profile does not match with the 2DH model, but that the erosion volume do match. Moreover, the improved agreement of the dune retreat suggest that the shape of the erosion profile is better captured with the reduced wave-group variation (Figure 3-11, panel C). This improved shape of the profile is not visible in the statistics of the erosion volumes, but this improvement could be important in the future when other parameters next to the erosion volume would play a role in the dune assessment.

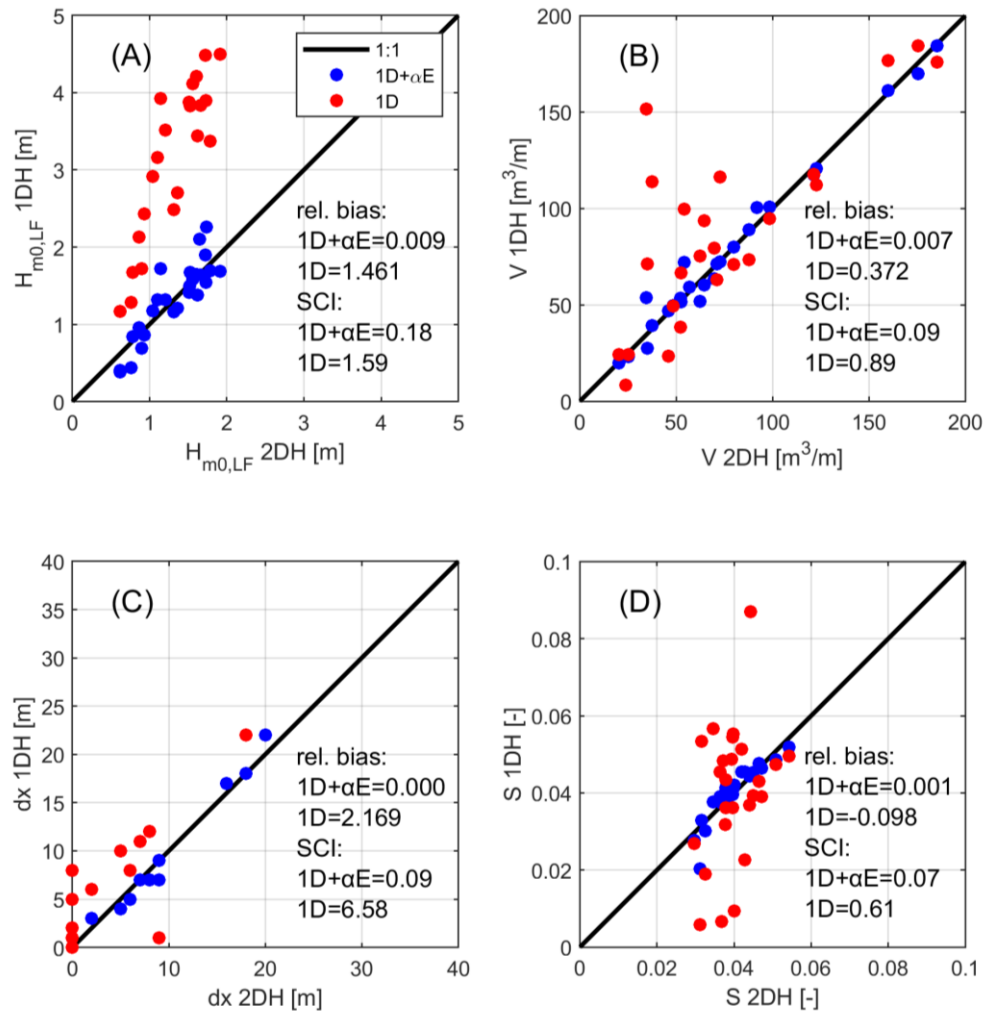


Figure 3-11: Scatter plot of 2DH results and 1DH results for all 26 representative profiles with an α_E parameter of 0.3 (blue) and 1 (red). The infragravity wave height is shown in panel A, the dune erosion volumes in panel B, the dune retreat in panel C and the foreshore slope in panel D. The relative bias (rel.bias) and the scatter index (SCI) for both the 1D and 1D+ αE are shown in each subplot.

Besides the relative bias and scatter index, the statistics of the speed-up factor and the erosion ratios are compared in a similar way as the other reduction approaches. The gain in computation time versus the loss in consistency is shown in Table 3-3. The mean difference in erosion volume relative to the 2DH results is very small for the modified 1D approach with 1.6% more erosion than in 2DH models and with a limited scatter of 15% standard deviation. Both the mean difference and scatter in erosion volume using the α_E reduction is significantly better than a regular 1D approach. The mean difference is 56% with a scatter of 117% standard deviation. Note that the mean and standard deviation of the erosion volume in Table 3-3 represent similar statistics as the relative bias and scatter index shown in Figure 3-11 (see Appendix B and Section 2.5).

Using the modified 1D approach, the computational time is significantly reduced compared to a 2DH model by a factor 60 (Figure 3-12 and Table 3-3). The modified 1D approach is also slightly faster than the 1D model. This difference is most likely caused by time step restrictions, which could result in a slightly larger timestep with the modified 1D approach. This larger time step is hypothesized to be the effect of smaller variations in the short-wave groups with the modified 1D approach, which result in slightly lower flow velocities and thereby in a larger time step.

Table 3-3: Overview of the relative gain in computational time (speed-up factor) versus the relative 'consistency loss' in calculating the erosion volumes based on the results of all 26 profiles forced with constant boundary conditions. The values are expressed in terms of the 2DH model result. Both gains and losses are represented with a mean and standard deviation. For the erosion volumes, also the spread over n number of profiles is provided. The spread for n=26 is calculated by taking the difference between the largest and smallest deviation in relative erosion volume. For n=22 and n=18, the 4 and 8 profiles with the largest (absolute) deviation in relative erosion volume are excluded respectively.

	Speed-up factor		Erosion volume				
	mean	std	mean	std	Spread		
					n=26	n=22	n=18
2DH	1,00	-	100,0%	-	-	-	-
1D	49	16	156,0%	117%	432.9%	256.2%	114%
Modified 1D	60	22	101,6%	14.5%	77.2%	18.5%	10.5%

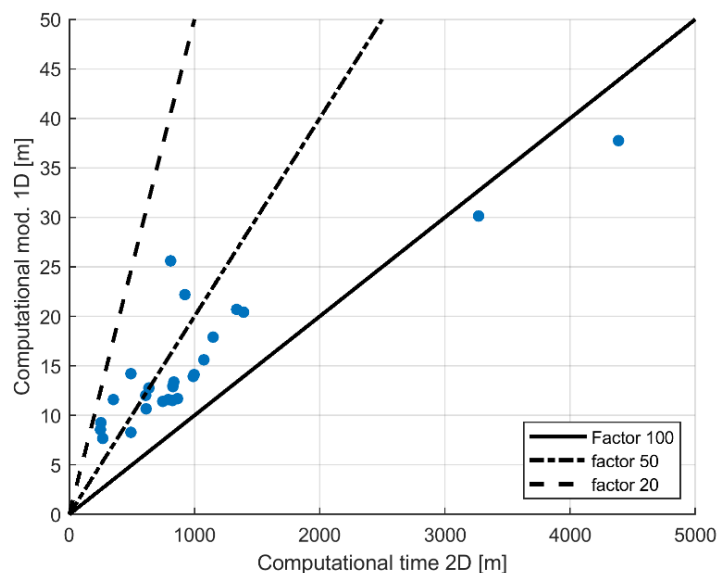


Figure 3-12: Scatter plot of the computational time in minutes with the 2DH model and the modified 1D approach.

3.5 Conclusions

In a 1D model the infragravity wave height is significant higher compared to an alongshore-uniform 2DH model (up to factor of 2.5) for a wave field with directional spreading. As a consequence, the dune erosion volumes are generally higher when a 1D model is applied. To prevent that a 1D model overestimates the infragravity wave height and dune erosion volumes, a reduction factor, α_E , is applied to the variance of the short-wave group signal at the boundary, while keeping the mean wave energy unchanged. Due to this reduction of the variation of the short-wave group signal the infragravity wave height growth is smaller and, thereby more comparable to an alongshore-uniform 2DH model with directional spreading. The modified infragravity wave height transformation compares better to the transformation in the alongshore-uniform 2DH case, and also influences the erosion volumes. When applying the reduction factor to the variance of the short-wave group signal, the erosion volumes are generally smaller and more comparable to an alongshore-uniform 2DH model.

It is found that a reduction of 70% in the wave group-variance ($\alpha_E = 0.3$), results in comparable results for the dune erosion, foreshore slope and dune retreat to an alongshore-uniform 2DH model for a large range of wave conditions when the directional spreading is greater than or equal to 30° (SCI of 0.02 and rel. bias of 0.001 for the dune erosion volumes). When the directional spreading is lower than 30° , the optimal α_E value is somewhat sensitive to the wave period and direction spreading and increases for a higher peak period and/or lower directional spreading. Since the wave conditions without much directional spreading are not very relevant for the storm conditions of the Dutch coast, this dependency is not included in recommendation for the BOI application.

The validation of this approach for 26 representative profiles of the Dutch coast show that the α_E approach significantly reduces the difference in nearshore infragravity wave height relative to an alongshore-uniform 2DH model (rel. bias 0.02 compared to 1.59). As a consequence, the erosion volumes are also more comparable to a 2DH model (rel. bias 0.006 compared to 0.32). Computation times for 1D models using the α_E approach are in the order of 60 times lesser than 2DH models. It is therefore concluded that the reduction of variance in the short-wave group signal is a good substitute for alongshore-uniform 2DH models in a transect-based assessment of the safety of the Dutch coast.

4 Morphological acceleration factor ‘*morfac*’

4.1 Introduction

The XBeach model has a built-in functionality to reduce the computational time by accelerating the morphological time scale with respect to the hydrodynamic time scale. The functionality is called morphological acceleration factor ‘*morfac*’ and it affects the simulation results through the processes of bed level updating and avalanching. By applying a *morfac*, all input time series and other time parameters are divided internally by *morfac*. Practically this means that water level time series are compressed and *morfac* times fewer waves are simulated. For example, if a *morfac* of 6 is applied, the model runs for 10 (hydrodynamic) minutes each hour. Bed level changes per timestep are then computed based on gradients in sediment transport, but multiplied with a factor 6 (equation 4.1, from XBeach Manual).

$$\frac{\delta z_b}{\delta t} + \frac{f_{mor}}{1 - \rho} \left(\frac{\delta q_x}{\delta x} \right) = 0 \quad (6.1)$$

in which z_b is the bed level, ρ is the porosity, f_{mor} is the morphological acceleration factor and q_x represents the sediment transport rate in x-direction.

In addition to the bed level changes due to gradients in sediment transports, bed levels can change when the slope exceeds a certain critical slope (which is different for dry and inundated areas). This process of avalanching is represented by equation 6.2. If a *morfac* is applied, the avalanching cycle is repeated *morfac* times each timestep.

$$\left| \frac{\delta z_b}{\delta x} \right| > m_{cr} \quad (6.2)$$

with m_{cr} representing a critical bed slope.

To make a decision on the *morfac*-value that can be applied in the dune safety assessment of 2023, the gains in computational time and the losses in performance of a range of *morfac* values are assessed in this chapter.

4.2 Approach

The 26 representative profiles introduced in chapter 2.2 are used to assess the effect of *morfac* on the XBeach performance. For each of the profiles, simulations are performed with the following *morfac*s: 1, 2, 3, 4, 5, 7.5, 10, 15 and 20. By comparing the results of higher *morfac*s with the results of the simulation with a *morfac* of 1 (i.e., no morphological acceleration), the gains in computational time and loss in accuracy are quantified.

The set of simulations is run with both constant and time-varying boundary conditions, more details in section 2.2.2. In both cases, 20 minutes of spin-up time were added to the simulations to assure that the waves reached the dune front before starting computing morphological change. In order to make a fair comparison between different *morfac* values, the spin-up time is multiplied with the *morfac* to make sure that the waves are fully developed in the model domain in the accelerated simulations.

A total of 468 simulations (26 profiles * 9 *morfac* values * 2 types of boundary conditions) are run. The results of these morphological predictions are assessed for the three morphological indicators; dune erosion volume, dune retreat and foreshore slope. These results are aggregated in order to focus on the overall effect of *morfac* on the morphological indicators.

The results of some profiles forced with constant boundary conditions are used as examples in the following paragraph, and the results for all individual profiles (with constant and time-varying boundary conditions) are presented in a supplementary document, see Appendix C.

4.3 Results

4.3.1 Constant boundary conditions

In Figure 4-1, the aggregated results for the simulations of all 26 profiles with constant boundary conditions and the full range of *morf* is presented. The upper panel in Figure 4-1 shows the speed-up factor of the computational time of the simulations with higher *morf*s, all with respect to the computational time of the simulation with a *morf* of 1. For *morf*s up to 5, the computational time reduces proportionally to the *morf*. However, for larger *morf*s, the spin-up time (which was multiplied with the *morf*) starts to become a significant part of the simulation period, which is reflected by a less than linear speed gain for increasing *morf*.

The other panels provide an indication of the consistency of XBeach results for variations in *morf*. Up to a *morf* of 5, the different morphological indicators for most of the profiles are within 10% with respect to the value obtained with a *morf* of 1. The number of profiles for which the morphological indicators deviate more than 10% from the results with a *morf* of 1, increases with increasing *morf* (in particular for *morf* values larger than 5).

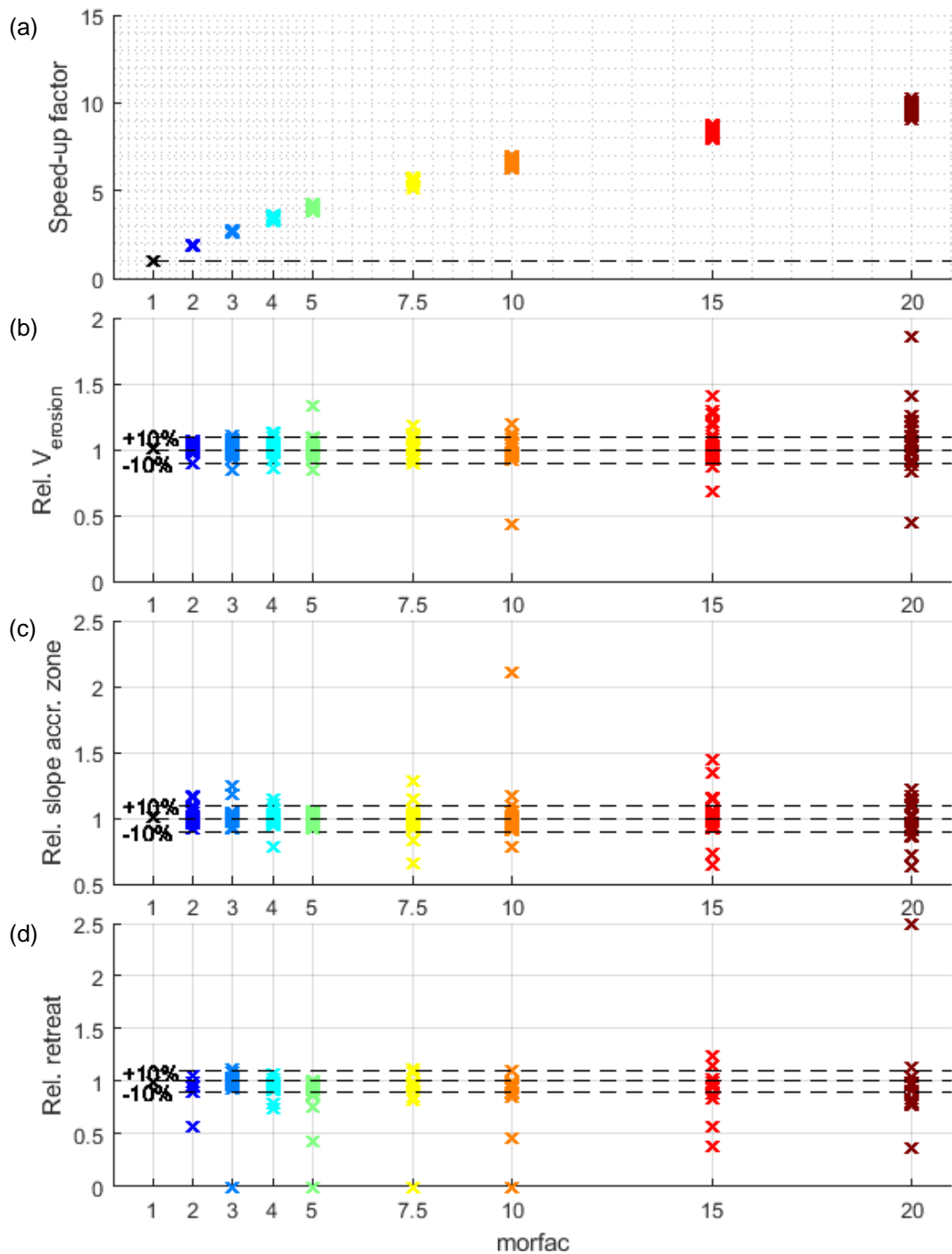


Figure 4-1: Aggregated overview of the results for all 26 profiles and all simulations forced with constant boundary conditions and with morfac larger than 1, relative to the results obtained with morfac 1, with in the upper panel (a) the speed-up factor (computational time), relative erosion volumes in the 2nd panel from above (b), relative slope of the accretion zone in the 3rd panel from above (c) and the relative dune retreat in the lower panel (d). Each 'x' indicates the result of a single simulation (i.e. a XBeach simulation of a single profile with a specific morfac).

Although in general XBeach results are relatively consistent for morfac's lower than 5, even for these low morfac's simulations are found that deviate more than 10% from the simulation with a morfac of 1. Note that such outliers found for a specific profile with for example a morfac of 3, do not necessarily mean that an outlier is found for the same profile with a morfac larger than 3. Based on analysis of all individual profiles (supplementary document, see Appendix C), three different explanations are found for these outliers:

- For some profiles, the modelled erosion volume is very limited. Small deviations in absolute erosion volumes will result in large relative deviations.
- There are a number of profiles for which XBeach predicts that the first dune row erodes completely, and thus overwash occurs. For these profiles, results obtained with higher morfac's tend to deviate more from morfac = 1 compared to profiles where only dune erosion occurs. Figure 4-2 shows an example of a profile that only experiences dune erosion, and an example where overwash occurs is presented in Figure 4-3. There, the simulation with a morfac of 15 predicts significantly less erosion (but still shows overwash occurring). Moreover, the profile obtained with a morfac of 20 differs significantly from the others, although the erosion volume is well predicted.
- The random wave seeding from a Jonswap spectrum could already result in ~2% deviation for simulations with a morfac of 1, see chapter 2.6. Analysis of the effect of random seeding for the set of varying morfac values (Figure A-9-1) has shown that the variation in morphological indicators increase with increasing morfac, hence this indicates the observed >10% deviation with respect to a morfac of 1.

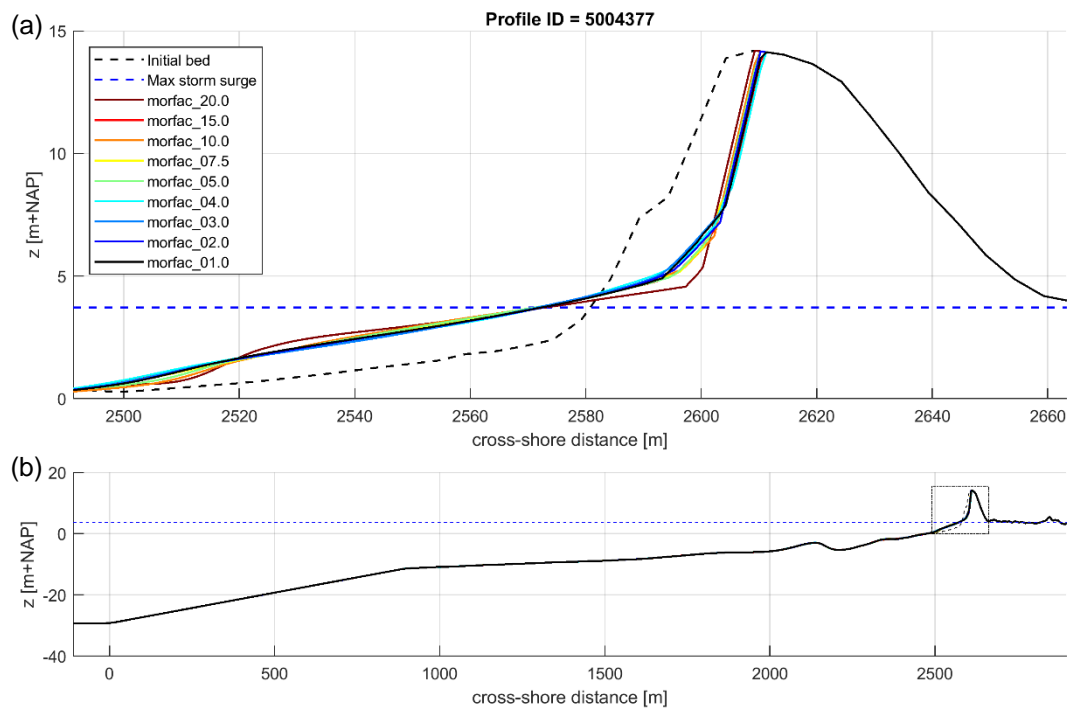


Figure 4-2: XBeach results for simulations with different morfac's for a profile (ID 5004377, Vlieland) in which only dune erosion occurs. In the lower panel (b), the entire model domain is shown with the bed level in black and the maximum storm surge level in dashed blue. The small rectangle in the lower panel indicates the extent of the zoomed view which is presented in the upper panel (a). The different colors in the upper panel represent the bed levels at the end of the simulations with different morfac's.

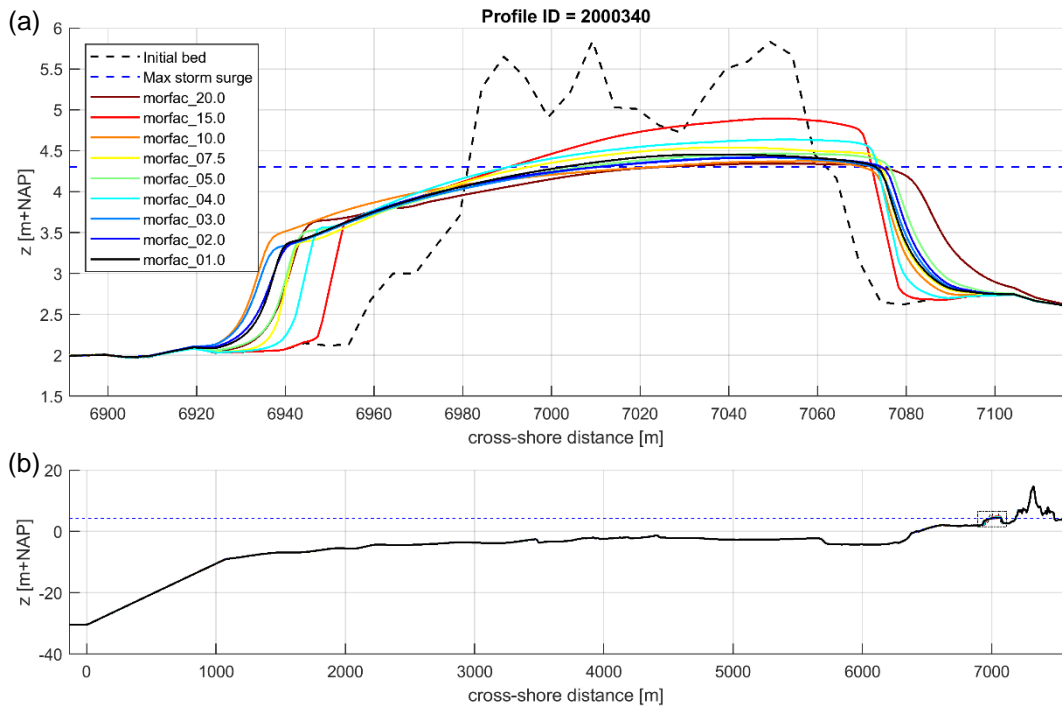


Figure 4-3: XBeach results for simulations with different morfac for a profile (ID 2000340, Schiermonnikoog) in which overwash occurs. In the lower panel (b), the entire model domain is shown with the bed level in black and the maximum storm surge level in dashed blue. The small rectangle in the lower panel indicates the extent of the zoomed view which is presented in the upper panel (a). The different colors in the upper panel represent the bed levels at the end of the simulations with different morfac.

Although some of the observed outliers can be explained, Figure 4-1 also shows that the spread in performance with respect to morfac 1 increases with increasing morfac. This qualitative observation is strengthened by the quantitative analysis provided in Table 4-1, which is focussed on the dune erosion volume indicator. For each morfac, the computational acceleration with respect to a morfac of 1 and averaged over the 26 profiles, is presented in the 2nd column as a speed-up factor. While increasing the morfac, the additional speed-up becomes smaller for morfac larger than 5. This is due to the spin-up time which is scaled with the morfac and hence becomes a significant part of the total simulation time for large morfac values. Furthermore, to indicate the uniformity over the 26 profiles in this acceleration, the spread around the mean speed-up factor is provided with the standard deviation, 3rd column in Table 4-1. For all morfac, this uniformity is large (standard deviation < 3% of the mean speed-up factor), indicating that the computational acceleration due to the morfac is equal for all profiles.

For the erosion volumes, again averaged over the 26 profiles and relative to a morfac of 1, the mean and standard deviation are presented (4th and 5th column), but also the spreads in consistency over n number of profiles are presented as additional measures of uncertainty. The spread for $n=26$ is the difference in relative erosion volume between the profiles with minimum and maximum deviation (considering all profiles), and the other spreads are defined in a similar way (only now a number profiles is excluded). In general, a slight increase in mean erosion volumes can be observed (with morfac = 10 as an exception) for increasing morfac values. The same holds for the uncertainty, which generally increases with increasing morfac (with an unexplained exception for morfac of 5). The spread provides more insight. Considering all profiles ($n=26$), a significant increase in spread is found for a morfac of 5. However, the spread for a morfac of 7.5 decreases again. When certain profiles with the largest deviations

are excluded from the analysis (e.g. n=22 or n=18), the spread over the simulations with a morfac of 5 reduces significantly (already for n=22). This is an indication that the large spread for n=26 is caused by only a few outliers. The spread for n=18 (hence excluding 8 profiles from the analysis) shows a clear increasing trend in uncertainty for increasing morfac.

Table 4-1: Overview of the relative gain in computational time (speed-up factor) versus the relative 'consistency loss' in calculating the erosion volumes based on the results of all 26 profiles forced with constant boundary conditions. All values for the simulations with higher morfacs are expressed with respect to the values found for simulations with morfac 1. Both gains and losses are represented with a mean and standard deviation. For the erosion volumes, also the spread over n number of profiles is provided. The spread for n=26 is calculated by taking the difference between the largest and smallest deviation in relative erosion volume. For n=22 and n=18, the 4 and 8 profiles with the largest (absolute) deviation in relative erosion volume are excluded respectively.

morfac	Speed-up factor		Erosion volume				
	mean	std	mean	std	Spread		
					n=26	n=22	n=18
1,00	1,00		100,0%				
2,00	1,89	0,03	101,1%	3,4%	17,7%	6,7%	5,4%
3,00	2,69	0,05	101,0%	5,3%	26,4%	11,3%	8,0%
4,00	3,43	0,07	101,5%	6,4%	27,7%	19,0%	8,8%
5,00	4,10	0,11	101,8%	8,2%	48,2%	12,5%	9,4%
7,50	5,51	0,15	102,8%	6,8%	28,9%	19,4%	10,2%
10,0	6,68	0,17	100,1%	13,3%	76,4%	16,3%	13,1%
15,0	8,46	0,22	104,0%	14,9%	71,9%	35,5%	24,2%
20,0	9,76	0,30	105,2%	24,1%	140,5%	37,8%	29,4%

4.3.2 Time-varying boundary conditions

The results for the simulations with time-varying boundary conditions are analysed in a manner similar to the simulations with constant boundary conditions. The aggregated results for the simulations of all 26 profiles with time-varying boundary conditions and the full range of morfac values are presented in Figure 4-4.

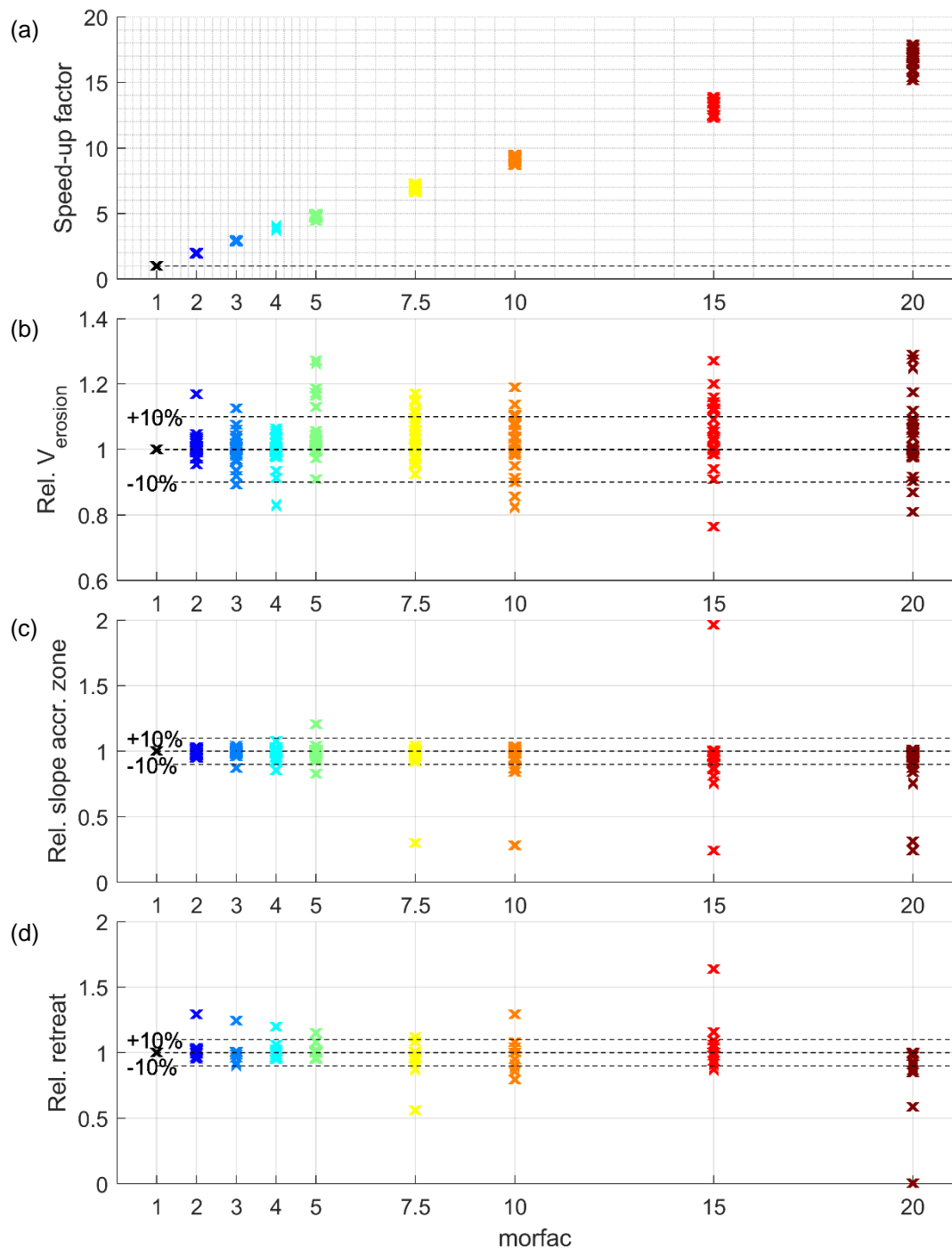


Figure 4-4: Aggregated overview of the results for all 26 profiles and all simulations forced with time-varying boundary conditions and with morfac larger than 1, relative to the results obtained with morfac 1, with in the upper pane (a) the speed-up factor (computational time), relative erosion volumes in the 2nd panel from above (b), relative slope of the accretion zone in the 3rd panel from above (c) and the relative dune retreat in the lower panel (d). Each 'x' indicates the result of a single simulation (i.e. a XBeach simulation of a single profile with a specific morfac).

In general, the simulations with time-varying boundary conditions correspond well to those with constant boundary conditions. Therefore, only the main differences in results between the two types of boundary conditions are discussed in this section.

At first, regarding the gain in computational time, it can be observed that the reduction in computational time is almost proportional to the morfac, even for higher morfacs. It was already stated that the spin-up time was the limiting factor in speeding up simulations with constant boundary conditions. However, the simulated time is now 32 hours (+20 minutes of spin-up) instead of 6 (+20 minutes of spin-up) for the constant boundary conditions, thus the relative contribution of the spin-up time becomes less important.

Secondly, where the mean erosion and its uncertainty generally increased for increasing morfac with constant boundary conditions, the results now can be divided into two parts. The mean erosion volumes for morfacs up to 4 are approximately equal to the mean erosion volume with morfac 1, and the accompanying uncertainty for morfacs up to 4 is low. For higher morfacs (5 and higher), the mean erosion volume deviates significantly (~5%) and also the accompanying uncertainty becomes approximately a factor 2 larger than for morfacs below 5.

Table 4-2: Overview of the relative gain in computational time (expressed in a speed-up factor) versus the relative 'consistency loss' in calculating the erosion volumes based on the results of all 26 profiles forced with time-varying boundary conditions.

morfac	Speed-up factor		Erosion volume				
	mean	std	mean	std	Spread		
					n=26	n=22	n=18
1,00	1,00		100%				
2,00	1,97	0,02	101,1%	3,9%	21,4%	6,4%	4,1%
3,00	2,93	0,03	100,6%	4,8%	23,2%	12,6%	7,3%
4,00	3,88	0,06	99,5%	4,7%	23,4%	11,4%	5,1%
5,00	4,80	0,11	105,6%	8,8%	36,4%	19,5%	16,6%
7,50	7,00	0,18	104,5%	7,2%	24,7%	19,4%	15,0%
10,0	9,14	0,24	102,2%	8,4%	36,4%	20,7%	15,0%
15,0	13,09	0,46	105,6%	10,2%	50,6%	21,8%	15,0%
20,0	16,78	0,74	104,1%	11,5%	47,9%	34,5%	14,3%

4.4 Conclusion

In general, the morphological acceleration factor is a powerful tool to speed-up computational time. Taking into account the results of the simulations with both constant and time-varying conditions, erosion volumes that deviate significantly more than 10% from the erosion volumes simulated with a morfac of 1 are first found for morfac values of 5. However, if profiles are excluded that are more sensitive to higher morfacs (e.g., profiles where overwash is expected), even higher morfac values could be taken into consideration.

5 Grid resolution and timestep

5.1 Introduction

The general model grid set-up presented in section 2.3 was based on previous experiences and recommendations within the BOI framework. However, that approach can be seen as a conservative base case since a high grid resolution in combination with a small time step are used. To make a decision whether the grid can be coarsened and/or the time step can be increased in the dune safety assessment of 2023, the gains in computational time and the losses in performance are assessed in this chapter for different grid resolution and timestep related parameters.

5.2 Minimum cross-shore grid size 'dxmin'

To be able to properly describe the dune front and morphological changes of the dune front, a minimum required cross-shore grid size '*dxmin*' can be defined when setting up a computational grid. The *dxmin* is thus usually applied over land, but the actual reference level above which this grid size is applied is 'user-defined' (see Figure 2-7 and section 5.3). The default value of *dxmin* is 1m. This section presents the results of simulations with varying values for *dxmin*.

The 26 representative profiles introduced in chapter 2.2 are used to assess the effect of *dxmin* on the XBeach performance. For each of the profiles, simulations are performed with the following values for *dxmin*: 0.5m, 1m (default), 1.5m, 2m, 3m, 4m and 5m. The set of simulations is only run with constant boundary conditions. Because *dxmin* is already applied for all grid cells above the minimum water level during storm conditions, it is not expected that time-varying boundary conditions result in different results.

A total of 182 simulations (26 profiles * 7 *dxmin* values * 1 types of boundary conditions) are run. The results of these morphological predictions are assessed for the three morphological indicators; dune erosion volume, dune retreat and foreshore slope. The results are aggregated for all 26 profiles in order to focus on the overall effect of *dxmin* on the morphological indicators. A graphical presentation of the aggregated results is presented in Figure 5-1 and the results are tabulated in Table 5-1.

In the upper panel of Figure 5-1, the speed-up factor for different *dxmin* values are depicted. The gain in computational time increases proportionally to increasing *dxmin*. However, the other panels show that both the simulated erosion volume and dune retreat are underestimated proportional to the increase in *dxmin*. Furthermore, for values of *dxmin* larger than 2m, the slope of the accretion zone for some profiles deviates significantly from the slope found with a *dxmin* of 1m.

Since the interest lies in speeding-up the XBeach simulations, the results obtained with a *dxmin* of 0.5m are not included in Figure 5-1 or Table 5-1. Nevertheless, the simulations showed that with a *dxmin* 0.5m instead of 1m, erosion volumes increased slightly (~4%), but also the computational times were on average 3 times longer. Moreover, XBeach model settings have been derived based on simulations with a *dxmin* of 1m. Furthermore, results of the current study show that a *dxmin* smaller than 1m is not necessary to capture the essential morphological changes in for example sensible profiles in which overwash occurs, see Figure 5-2.

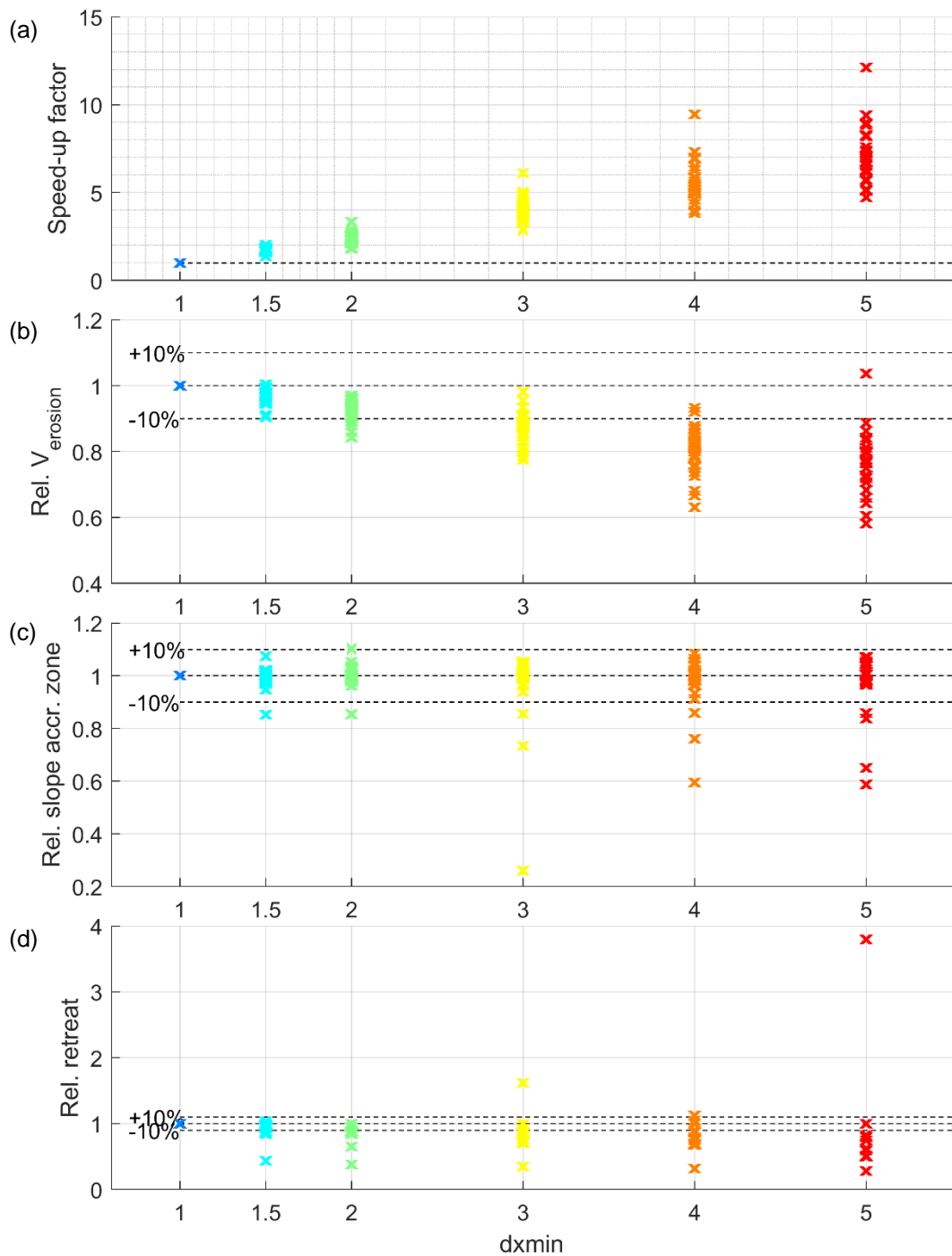


Figure 5-1: Aggregated overview of the results for all 26 profiles forced with constant boundary conditions while different dx_{min} is used for grid generation. Results of the various simulations are expressed relative to the simulation with default $dx_{min} = 1m$. The upper panel (a) shows how many times faster the computation becomes with respect to the default, relative erosion volumes are shown in the 2nd panel from above (b), relative slope of the accretion zone in the 3rd panel from above (c) and the relative dune retreat in the lower pane (d). Each 'x' indicates the result of a single simulation (i.e. a XBeach simulation of a single profile with a specific dx_{min}).

Table 5-1: Overview of the relative gain in computational time (expressed in a speed-up factor) versus the relative 'consistency loss' in calculating the erosion volumes based on the results of all 26 profiles for simulations with varying dxmin.

Dxmin	Speed-up factor		Erosion volume				
	mean	std	mean	std	Spread		
					n=26	n=22	n=18
1,0 m	1,00		100,0%				
1,5 m	1,71	0,15	96,5%	2,4%	10,0%	5,0%	4,5%
2,0 m	2,47	0,32	92,8%	3,3%	12,8%	8,3%	6,1%
3,0 m	4,04	0,69	87,0%	5,2%	20,8%	15,0%	10,0%
4,0 m	5,60	1,17	80,3%	7,3%	30,2%	19,7%	12,9%
5,0 m	7,07	1,57	76,8%	9,4%	45,4%	21,8%	15,1%

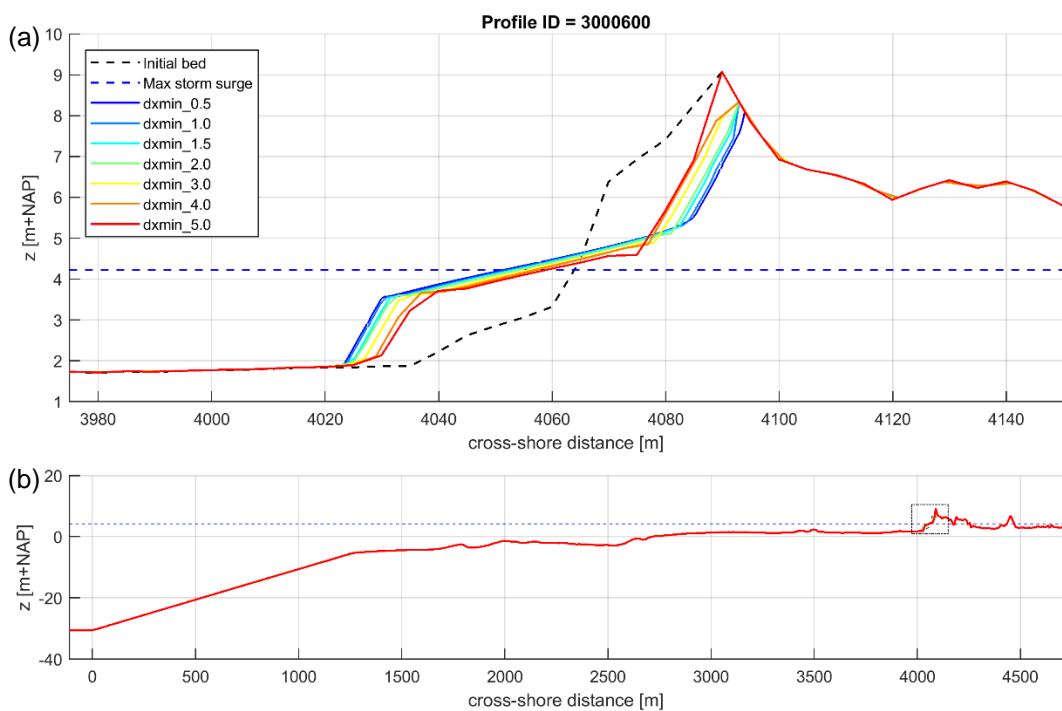


Figure 5-2: Example XBeach results using grids with varying dxmin for a profile in which overwash events occur. For large dxmin, the impact of overwash events are underestimated. The small rectangle in the lower panel (b) indicates the extent of the zoomed view which is presented in the upper panel (a).

5.3 Elevation above which *dxmin* is applied

The minimum grid size in cross-shore direction is applied above a certain level. In the default approach, this level is defined at the minimum water level during storm conditions. However, losses in bed elevation are only considered as dune erosion for elevations above maximum storm surge level. This section presents the results of simulations in which the elevation above which 'dxmin' is applied has been varied between: the minimum water level during the storm; the dune foot level for the Dutch coast (set at NAP + 3m) to ensure the grid resolution on the dune front is always equal to 'dxmin'; and the maximum water level during the storm, such that the minimum cross-shore resolution is only used in the area that coincides with that used to compute the dune erosion volume (Figure 2-8).

In contrast to the previous section, simulations with time-varying conditions (especially varying water level) could be more sensitive to changing this reference level. Therefore, the simulations in this section are performed with both constant and time-varying boundary conditions. A total of 156 simulations (26 profiles * 3 *water level* values * 2 types of boundary conditions) are run. The results are assessed in a similar way as in section 5.2. The aggregated results for the simulations with constant and time-varying boundary conditions are tabulated in Table 5-2 and Table 5-3, respectively.

For both constant and time-varying boundary conditions, increasing the reference level above which *dxmin* is applied has minimal impact on simulated the erosion volumes. Increasing the reference level to NAP+3m speeds-up the computations on average by about 2 times, whereas the mean predicted erosion volume only deviates 0.1%. When also considering the various spreads, no profiles are found for which the erosion volume deviates more than 5%. Further increasing the reference level towards the maximum storm surge level results in a further acceleration of the computation (speed-up factor ~3-4). Erosion volumes for all profiles remain within the 10% bandwidth with respect to the base case simulations. Increasing this reference level is thus an efficient way of speeding-up the simulations without losing accuracy.

Table 5-2: Overview of the relative gain in computational time (expressed in a speed-up factor) versus the relative 'consistency loss' in calculating the erosion volumes based on the results of all 26 profiles forced with constant boundary conditions. Each row represents a different set of simulations. For each set of simulations, a different water level has been used above which the minimum required grid size dxmin is applied.

Water level	Speed-up factor		Erosion volume				
	mean	std	mean	std	Spread		
					n=26	n=22	n=18
Min (default)	1		100,0%				
NAP+3m	1,70	0,30	99,9%	1,5%	7,0%	3,1%	2,1%
max	2,80	0,94	100,2%	2,1%	11,8%	4,3%	2,1%

Table 5-3: Overview of the relative gain in computational time (expressed in a speed-up factor) versus the relative 'consistency loss' in calculating the erosion volumes based on the results of all 26 profiles forced with time-varying boundary conditions. Each row represents a different set of simulations. For each set of simulations, a different water level has been used above which the minimum required grid size dxmin is applied.

Water level	Speed-up factor		Erosion volume				
	mean	std	mean	std	Spread		
					n=26	n=22	n=18
min (default)	1,00		100,0%				
NAP+3m	2,09	0,53	100,1%	1,7%	7,8%	3,9%	3,0%
max	4,40	2,10	101,3%	4,5%	18,1%	12,5%	7,9%

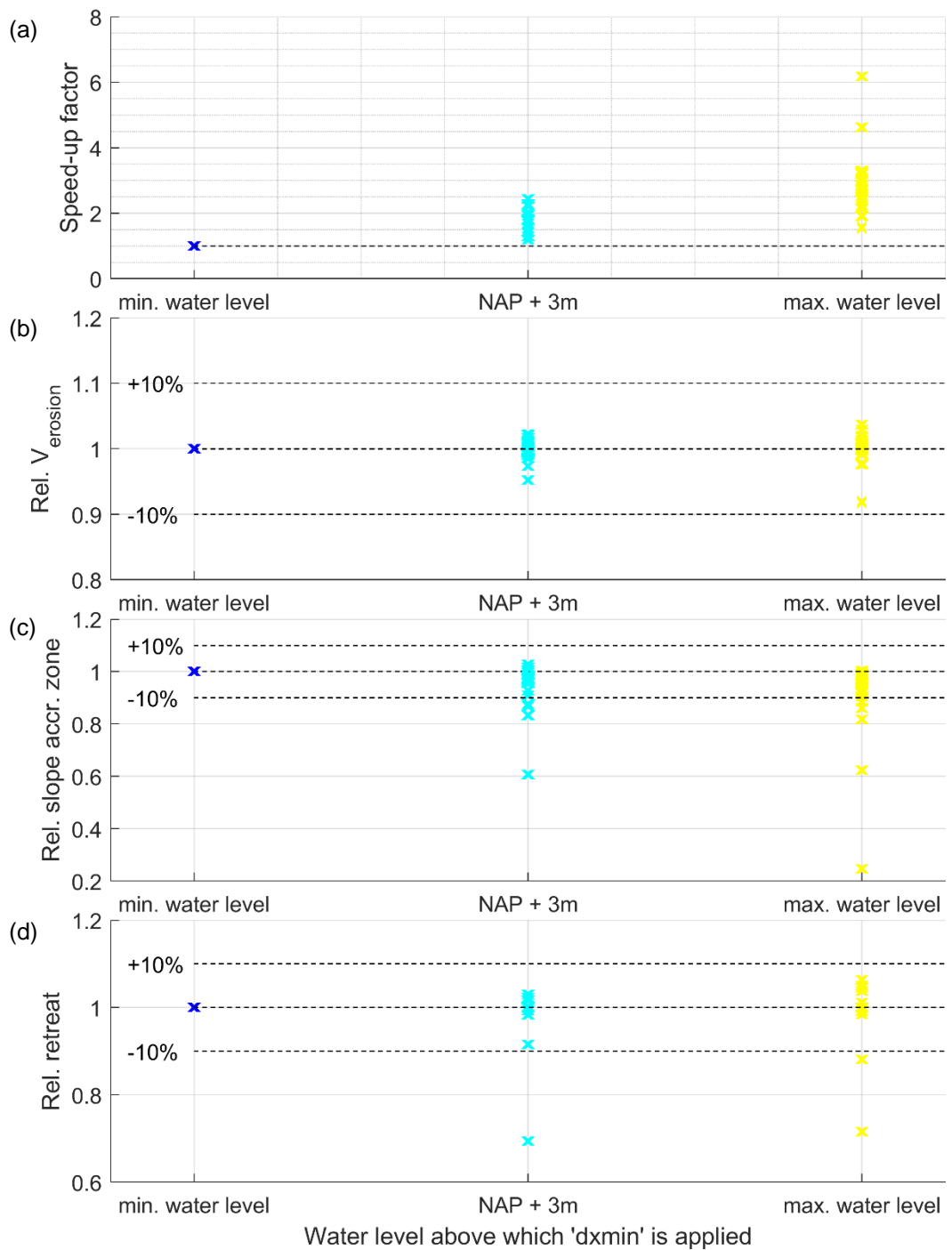


Figure 5-3 Aggregated overview of the results for all 26 profiles forced with constant boundary conditions while different water levels are used above which dxmin is applied during grid generation. Results of the various simulations are expressed relative to the base case simulation. The upper panel (a) shows how many times faster the computation becomes with respect to the default. Relative erosion volumes are shown in the 2nd panel from above (b), relative slope of the accretion zone in the 3rd panel from above (c) and the relative dune retreat in the lower panel (d). Each 'x' indicates the result of a single simulation (i.e. a XBeach simulation of a single profile with a specific water level above which dxmin is applied).

5.4 Number of points per wavelength

Where dx_{min} restrains the grid size on the landward side of the model domain, the number of points per wavelength affects the grid resolution towards the offshore boundary. Based on previous experiences, 40 points per wave group length ($ppwl$) is used in the base case simulations. This section presents the results of simulations with varying values for $ppwl$.

The 26 representative profiles introduced in chapter 2.2 are used to assess the effect of $ppwl$ on the XBeach performance. For each of the profiles, simulations are performed with the following values for $ppwl$: 12, 20, 30, 40 (default) and 50. The set of simulations is only run with constant boundary conditions. A total of 130 simulations (26 profiles * 5 dx_{min} values * 1 types of boundary conditions) are run. The results aggregated over all 26 profiles are presented in Figure 5-4 and Table 5-4.

The upper panel of Figure 5-4 shows the speed-up factor for the simulations with varying points per wave group length. Note that the limits of the y-axis are much smaller than in previous shown panels with speed-up factors. Decreasing the number of points per wavelength ultimately results in a speed-up factor of 1.14 (for a single profile and the lowest points per wave group length). Compared to this relatively small gain in computational time, some significant outliers are found in the panels representing the morphological indicators. Further analysis of these outliers shows that these outliers are mainly found for profiles in which overwash occurs. For a small number of points per wavelength, the morphological effects of overwash events deviate significantly from simulations with 40 (default) or more points per wave group length, see Figure 5-5.

Table 5-4 clearly shows that decreasing the number of points per wave group length hardly speeds-up the computations (<5%), whereas the uncertainty in the predictions of the erosion volumes increases by the same amount. Therefore, it is not considered worthwhile to reduce the number of points per wave group length in order to speed-up the computations.

Table 5-4: Overview of the relative gain in computational time (expressed in a speed-up factor) versus the relative 'accuracy loss' in calculating the erosion volumes based on the results of simulations with different minimum points per wavelength($ppwl$) for all 26 profiles forced with constant boundary conditions.

PPWL	Speed-up factor		Erosion volume				
	mean	std	mean	std	Spread		
					n=26	n=22	n=18
12	1,05	0,03	101,0%	6,5%	35,2%	8,0%	4,8%
20	1,04	0,03	102,6%	8,9%	41,1%	6,3%	5,0%
30	1,03	0,02	101,5%	3,8%	20,4%	7,5%	2,7%
40	1,00		100,0%				
50	0,97	0,01	99,7%	1,7%	9,1%	3,6%	2,3%

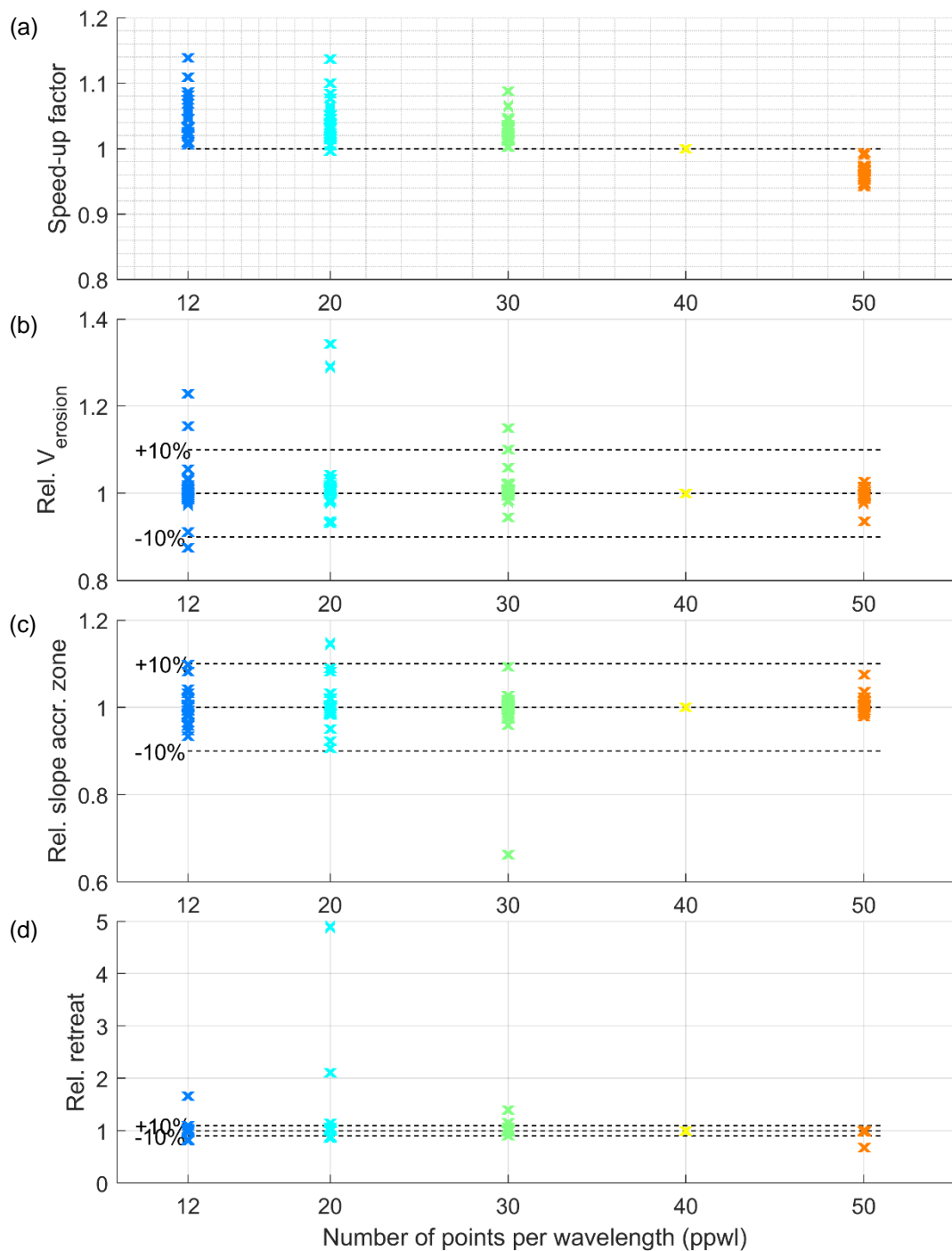


Figure 5-4: Aggregated overview of the results for all 26 profiles forced with constant boundary conditions while different ppwl is used for grid generation. Results of the various simulations are expressed relative to the simulation with default ppwl = 40. The upper panel (a) shows how many times faster the computation becomes with respect to the default, relative erosion volumes are shown in the 2nd panel from above (b), relative slope of the accretion zone in the 3rd panel from above (c) and the relative dune retreat in the lower panel (d). Each 'x' indicates the result of a single simulation (i.e. a XBeach simulation of a single profile with a specific ppwl).

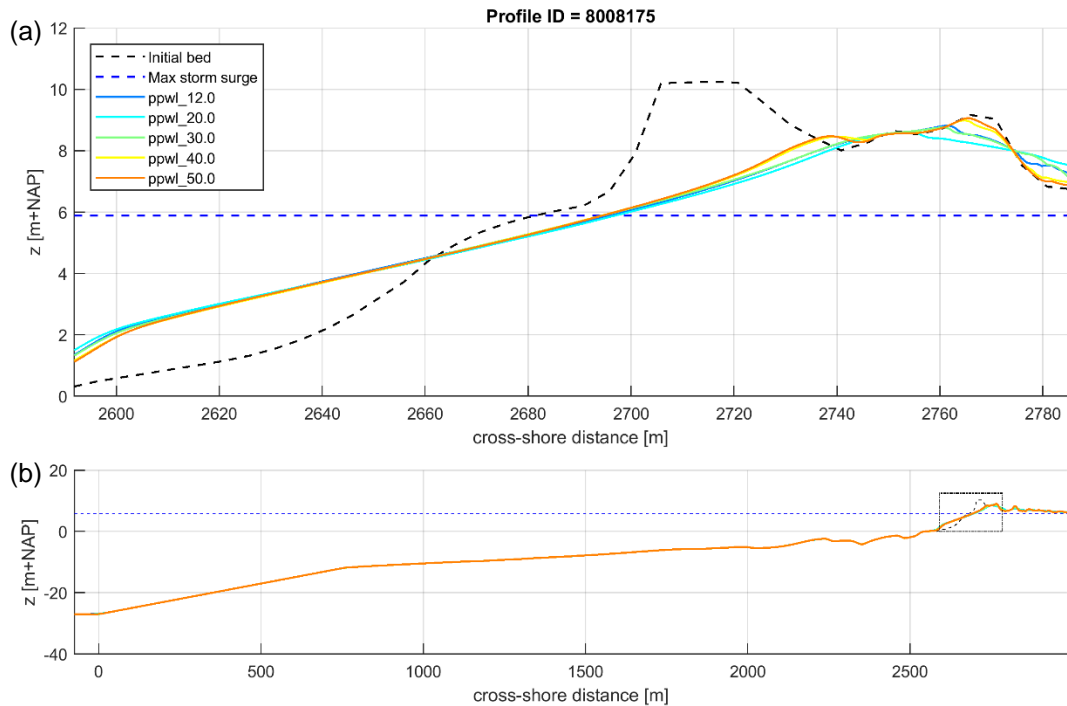


Figure 5-5: Example XBeach results for profileID 8008175 using grids with varying ppwl for a profile in which overwash events occur. For a small number of points per wave group length, the morphological effects of overwash events deviate significantly from simulations with 40 (default) or more points per wave group length. The small rectangle in the lower panel (b) indicates the extent of the zoomed view which is presented in the upper panel (a).

5.5 Time step

A potential reduction approach is the time step, since a larger time step requires fewer computations (number of timesteps) to reach the end time of the simulation. The applied time step is constrained by the stability criteria of the numerical scheme. XBeach applies an explicit numerical scheme for the time discretisation, which means that the time step is constrained by the Courant number (CFL condition). To prevent numerical instabilities, the courant number must be smaller than 1. Based on the model results of each time step, XBeach automatically determines the required time step based on the courant number. Thus, to optimize the computational time, the CFL condition can be varied. Since, the implemented Courant conditions in XBeach is derived for two-dimensional models, the applied courant condition can be too restrictive for one-dimensional models. Therefore, the CFL condition is varied from 0.7 (default) to 1.5.

The effects of varying the CFL condition and, thereby, the timestep are shown in Figure 5-6. The results show a large dependency of the CFL condition on the computational time. Varying the CFL from 0.7 to 1.5 result in a factor 2 in computational time. However, above a value of 1, the morphological indicators show a different result for the 26 profiles. The erosion volumes become 6 times larger when a CFL condition of 1.5 is applied. A closer inspection of the simulation results also show wiggles in the water level and bed level (not shown), which indicates that the model is not fully stable anymore.

Below a CFL value of 1 all the morphological indicators show a similar result as the base case. Dune erosion volumes deviate less than 10% with the base case when the CFL condition is lower than 1.

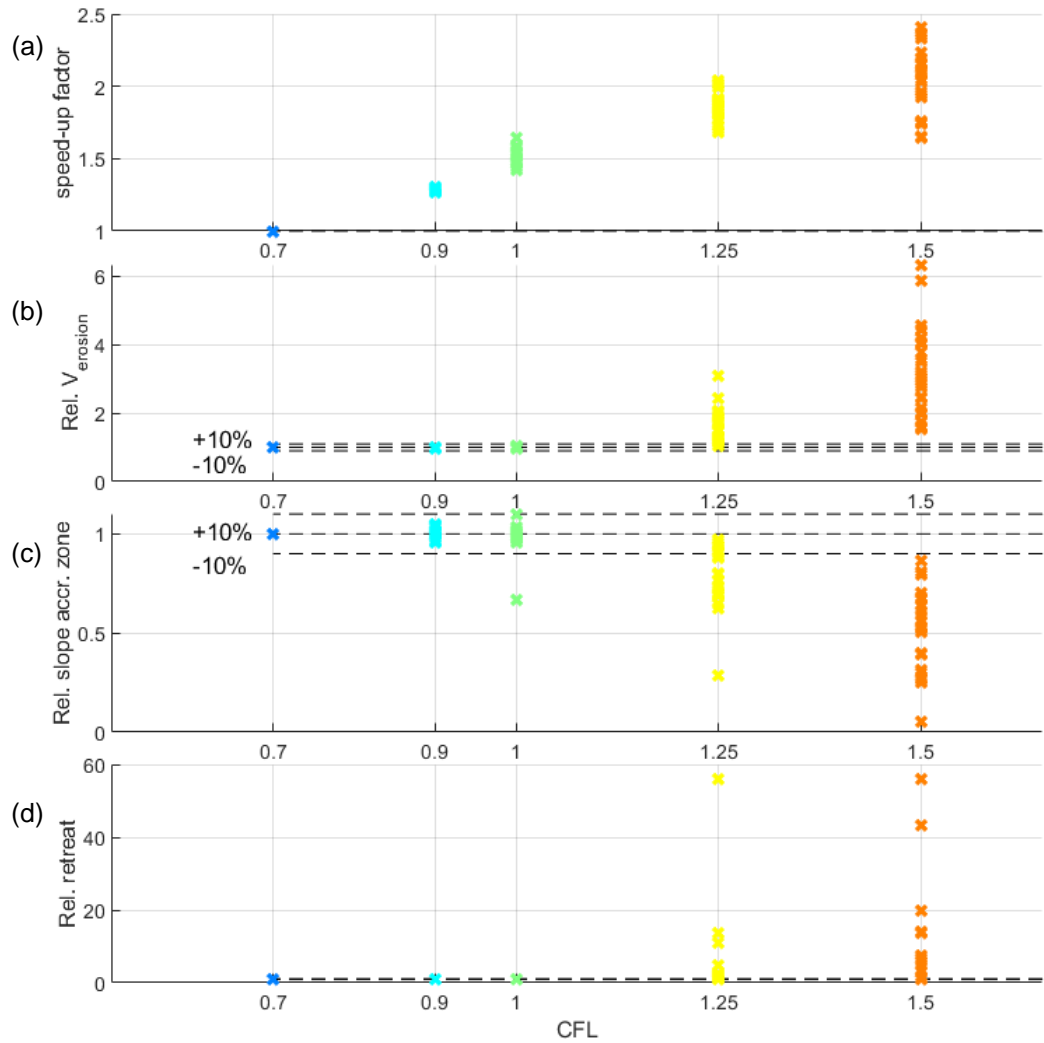


Figure 5-6: Aggregated overview of the results for all 26 profiles forced with constant boundary conditions while different CFL conditions is used for grid generation. Results of the various simulations are expressed relative to the simulation with default CFL = 0.7. The upper panel (a) shows how many times faster the computation becomes with respect to the default, relative erosion volumes are shown in the 2nd panel from above (b), relative slope of the accretion zone in the 3rd panel from above (c) and the relative dune retreat in the lower panel (d).

Table 5-5: Relative gains and loss in consistency for simulations with constant boundary conditions for different CFL conditions.

CFL	Speed-up factor		Erosion volume				
	mean	std	mean	std	Spread		
					n=26	n=22	n=18
0.7	1,00		100%				
0.9	1,19	0,35	100%	1%	5,0%	2,6%	1,8%
1.0	1,50	0,05	100%	2%	8,0%	4,2%	2,5%
1.25	1,86	0,11	160%	45%	202,8%	92,3%	72,7%
1.5	2,04	0,24	319%	125%	478,8%	295,7%	220,3%

5.6 Conclusion

- A dx_{min} of 1m is small enough to capture the relevant processes. Increasing the grid size results in an underestimation of the erosion volumes which can be estimated roughly with dx_{min} times the erosive height.
- By increasing the reference level above which dx_{min} is applied, computations can be accelerated up to a factor 4, whereas the predicted erosion volumes remain within the 10% bandwidth with respect to the erosion volumes predicted in the base case simulations.
- Decreasing the number of points per wave group length hardly speeds-up the computations (<5%), whereas the uncertainty in the predictions of the erosion volumes increases with the same order of magnitude. Therefore, it is not worthwhile to reduce the number of points per wavelength in order to speed-up the computations.
- The simulations with a varying Courant condition (CFL) show that the model provides consistent results for CFL values less than or equal to 1 (less than 10% deviation). The computational time is a factor 1.5 faster when the CFL is increased from 0.7 (base case) to 1.0.

6 Single precision

6.1 Introduction

The XBeach source code is programmed with double-precision variables (64 bits), but a XBeach code with single-precision (32 bits) could be sufficient. Only when an extreme precision of fractional numbers is required or when a wide range of numbers is applied, is the double-precision format preferable. Therefore, a branch of the BOI XBeach model with a source code programmed in single-precision is developed to test whether that would increase the computational speed.

To test the potential reduction in computational time, both the XBeach executables compiled with the source code in single and double-precision are applied for the 26 representative profiles. Since the single-precision version of XBeach requires also boundary conditions in single-precision, the simulations are including generation of the boundary conditions. This means that the random seeding effect is visible in the result due to a random wave signal.

6.2 Effect of single-precision

When the computational times are compared between the simulations of the two executables, the reduction in computational time is negligible (see Table 6-1). Apparently, the computational time of XBeach is not affected by the variable format. The XBeach computation is even slightly slower than the base case, but this could also be caused by the wave seeding effect since the two variations are not computed with the same boundary condition.

Table 6-1: Relative gains and consistency losses for simulations with constant boundary conditions for simulations computed with a single precision XBeach and a double-precision XBeach.

	Speed-up factor		Erosion volume				
	mean	std	mean	std	Spread		
					n=26	n=22	n=18
Base case	1.00		100%				
Single-precision	0.98	0.069	99.7%	3.5%	17,4%	8,3%	4,7%

6.3 Conclusion

A XBeach version with the single-precision format was programmed to verify the effects of the variable format is on the computational time. When the simulations of both a XBeach version with single precision and double precision are compared, the differences in computational time and output is negligible. Thus, a XBeach source code with single-precision shows the same results as a XBeach source code with double-precision, but it has no effect on the computational time.

7 Combined approaches and computation times

The previously described results show how the individual approaches affect computational time and consistency of XBeach. To verify whether the relation found between the consistency of model results and computational time also holds for a combination of reduction approaches, the most important reduction approaches are combined.

The following adjustments are applied with respect to the base case to test the combined effect:

- A modified 1D approach, accounting for wave directional spread effects, instead of 2DH;
- applying a (slightly conservative) *morfac* of 4;
- vertical reference level for the minimum grid size is set to NAP + 3 m (approximate dune foot position for the Netherlands);
- and the CFL condition is changed from 0.7 to 1.

These variations are selected based on a maximum accuracy deviation of approximately 10%. Note that this selection is not directly a recommended selection for the dune safety assessment of 2023, but merely a test to quantify the potential effect on the computational expense and model accuracy.

In the 2DH models it takes on average ~2.8 hours of computational time (varying from min 0.7h to max 12.2h) for a 1-hour simulation period (Table 7-1). First, application of a modified 1D approach will reduce computational time to ~2,5 minutes (varying from min 1,3 to max 6,3 min) per 1-hour simulation period. The other three adjustments to the modified 1D approach will result in a ~20 seconds (varying from min 10 to max 41 s) calculation time per 1-hour simulation period. Altogether, this is a reduction in computational time of a factor 500 on average (Figure 7-1, left panel), which is the combined effect of a modified 1D approach with respect to 2DH (factor ~50) and the accelerations to the 1DH approach (factor ~10), see Table 7-2.

The reduction in computational time does not result in a significant loss of the accuracy. All the 26 profiles show a deviation in the dune erosion volume of, on average, less than 10% (Figure 7-1, right panel). This is also reflected by the modelled post-storm profiles (Figure 7-2), the results with the accelerated modified 1D are highly similar to the 2DH results.

The above absolute and relative values on computational effort and accuracy are based on the simulations with constant boundary conditions. For the time-varying boundary conditions similar reduction factors for computational time are found, i.e. a factor ~10 due to the improvements to the accelerated modified 1D approach (Figure 7-3, left panel). Again, the uncertainty in the modeled dune erosion volumes stays well within the 10% with respect to the regular 1D approach.

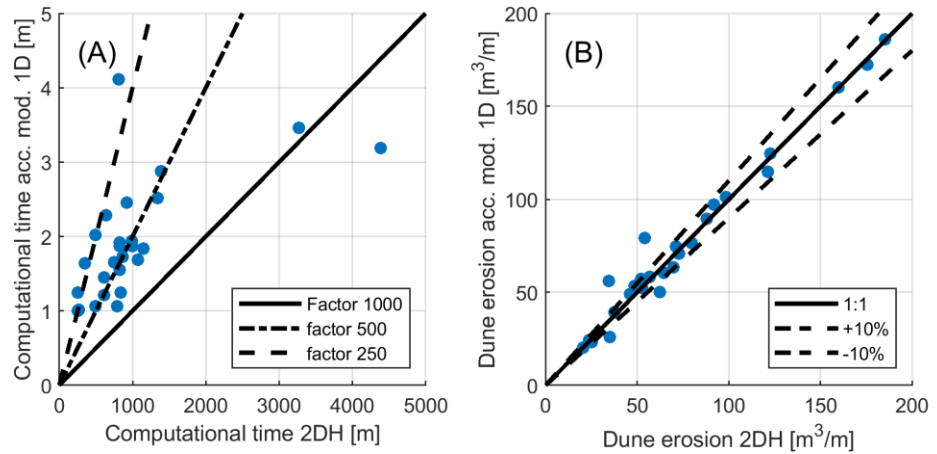


Figure 7-1: Scatter plot of computation time (panel A) and dune erosion volumes (panel B) between the 2DH base case and the accelerated modified 1D approach for the 26 representative profiles with constant boundary conditions.

Table 7-1: Characteristics of the computational time in seconds and erosion volumes in m³ for the 2DH, 1D and 1D+adjustments simulations with 26 representative profiles forced with constant boundary conditions (6 hour simulation).

	Computational time [s]				Erosion volume [m ³]			
	mean	std	min	max	mean	std	min	max
2DH	60.000	53.980	15.010	2.632.400	-74,98	45,30	-20,32	-185,22
Modified 1D	920,9	425,1	461,5	2263,4	-75,48	44,66	-19,74	-184,49
Accelerated modified 1D	115,2	47,4	60,2	246,7	-76,14	44,75	-20,17	-185,89

Table 7-2: Relative speed-up factor for the 2DH, 1D and 1D+adjustments simulations (mean and standard deviation), versus the relative 'accuracy loss' in calculating the erosion volumes based on the results of all 26 profiles forced with constant boundary condition (6 hour simulation)s.

	Speed-up factor		Erosion volume				
	mean	std	mean	std	Spread		
					n=26	n=22	n=18
2DH	1	-	100,0%	-	-	-	-
Modified 1D	60	22	101,6%	14,5%	77,2%	18,5%	10,5%
Accelerated modified 1D	493	254	103,0%	17,3%	88,8%	19,4%	13,0%

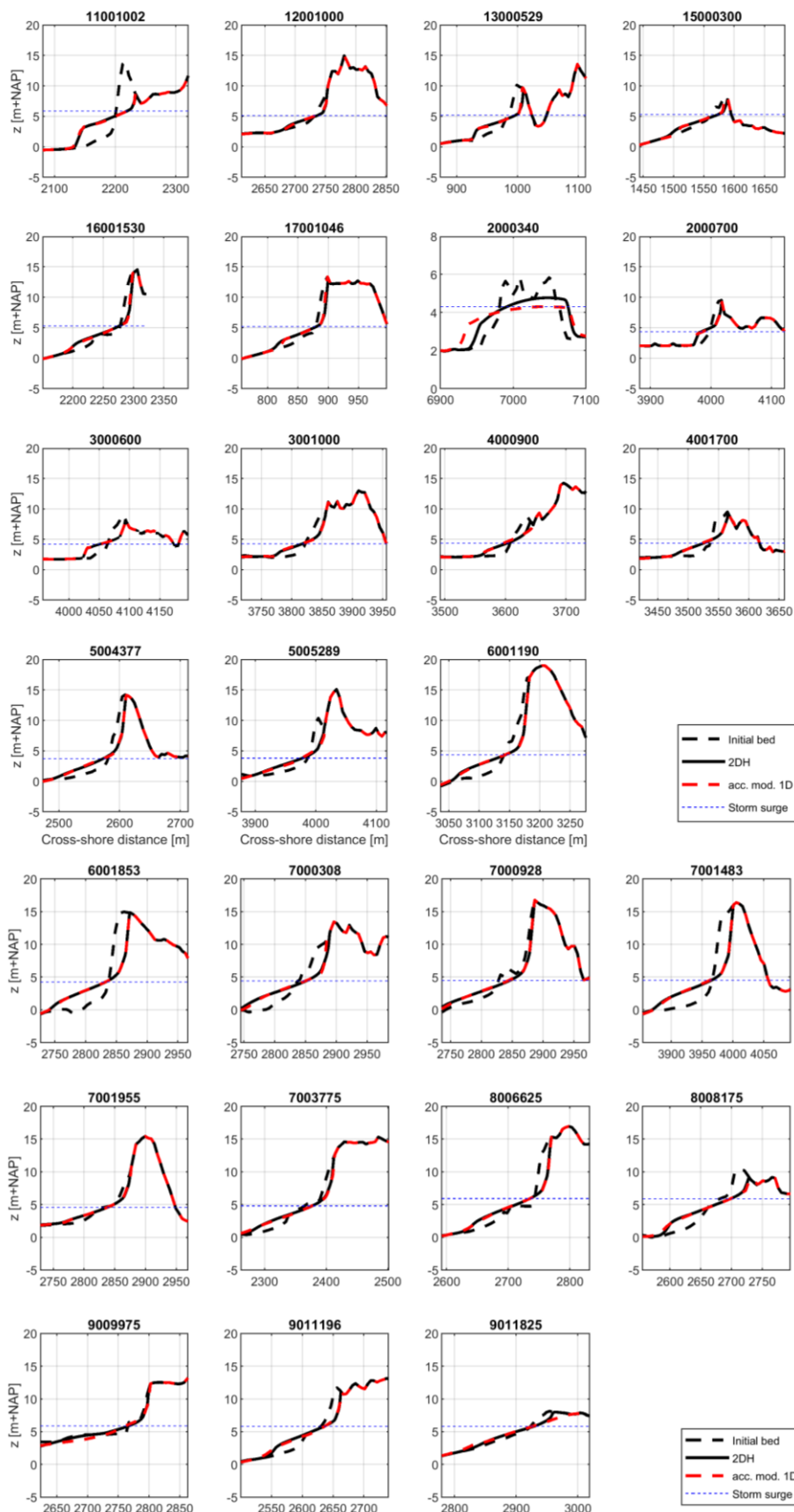


Figure 7-2: Overview of the profiles obtained with the 2DH approach (black) and accelerated modified 1D approach (dashed red, acc. Mod. 1D). The initial bed level is shown with a dashed black line and the storm surge with a blue dashed line.

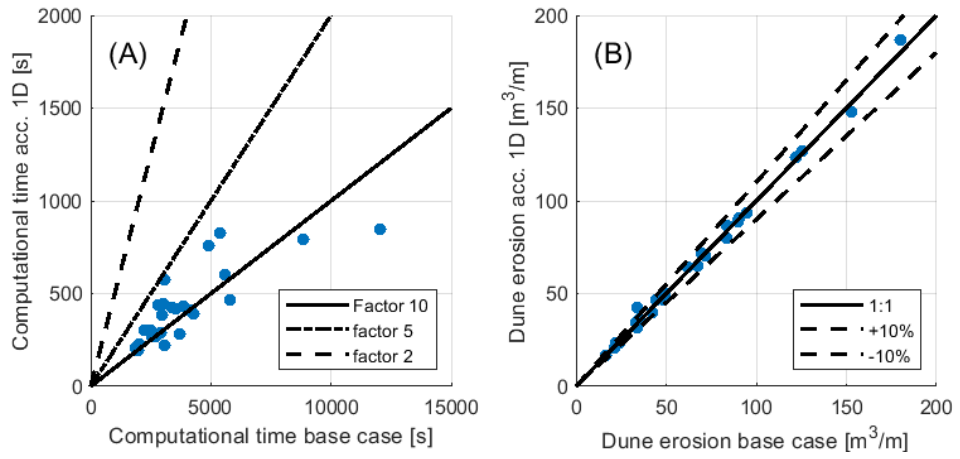


Figure 7-3: Scatter plot of computation time (panel A) and dune erosion volumes (panel B) between the 1D base case and the accelerated 1D approach for the 26 representative profiles with time-varying boundary conditions.

8 Conclusions and recommendations

8.1 Conclusions

The main research question of the study is: “*What approaches can be applied to reduce computational time in XBeach, significant loss of consistency in predicted results?*”

The first approach that reduces computational time significantly with a factor ~60 is applying a modified one-dimensional (1D) approach instead of two-dimensional (2DH). The predictions of the 1D XBeach model are now consistent with an alongshore-uniform 2DH model approach by parametrically accounting for the effects of directional spreading in a 1D XBeach approach. In addition, three acceleration approaches are found that provide a significant reduction in computational time and small loss in accuracy; applying a morphological acceleration factor (*morfac*), optimizing the location of the minimum grid resolution and increasing the time step. Altogether, this accelerated modified 1D approach leads to a reduction in computational time of a factor 500 with respect to the 2DH approach.

The conclusions on the four investigated approaches, and corresponding sub questions, are listed in more detail below.

- 1 *Can directional spreading be included in a one-dimensional model, in order to be consistent with an alongshore-uniform two-dimensional model?*

The overestimation of infragravity wave height and dune erosion volumes in a 1D model described in Deltares (2020) has been removed by the implementation of a reduction factor (parameter α_E) on the variance of the short-wave group signal at the boundary. It is found that a reduction of 70% in the wave group-variance, while maintaining the mean wave height, results in comparable results to a 2DH model. This is valid for a large range of wave conditions if the directional spreading is greater than 30°, which is typical for the types of conditions to be applied in the Dutch dune safety assessment. For the 26 representative profiles it is shown that predictions of nearshore infragravity wave height and dune erosion volume are significantly improved (i.e., more similar to the 2DH model results) using the α_E reduction factor, compared to simple 1D model results. The gain in computational time using the modified 1D approach compared to a 2DH model is significant, with computational times reduced on average by a factor 60.

- 2 *How much can a morphological acceleration factor reduce computational time without significant deviations in model accuracy?*

Application of a morphological acceleration factor (*morfac*) is a known measure to reduce computational time, but one that can also affect model results. When applying a morphological acceleration factor in XBeach, the simulation period is reduced by a factor *morfac* and computed bed level changes are multiplied by a factor *morfac*. For instance, using a *morfac* of 10, a 40-hour storm is simulated in XBeach with 4 hours of hydrodynamics, but computed bed level changes are amplified by 10. Application of high *morfac* values is limited by the ability of the model to accurately represent hydrodynamic processes and morphodynamic interactions well.

Generally, XBeach performs well for *morfac* lower than 5, and shows an almost linear reduction in computational time. For higher *morfac* (5 and higher), the mean erosion volume deviates more (~5%). Also, the spin-up time (which was multiplied with the *morfac*) starts to become a significant part of the simulation period, which is reflected by a lower increase in speed-up factor for increasing *morfac*.

Generally, it is observed that for profiles for which XBeach predicts overwash, i.e. the first dune row is eroded completely, results are more sensitive for higher *morfac* values.

3 *What temporal and spatial discretisation can be applied to optimize the computational time without losing model accuracy?*

Optimizing the grid resolution is found to be a straightforward measure to reduce computational expense up to a factor 4, particularly by optimizing the vertical reference level where the minimum grid size should be applied. This reduces the total number of grid cells, especially for mildly sloping profiles in the Wadden Islands, and therefore the computational time. The loss in accuracy for erosion volumes are within 4,5% compared to the baseline. Other measures such as increasing nearshore minimum grid size or offshore maximum grid size also decrease computational time but come with a significant reduction in model skill.

The time step in XBeach is constrained by the Courant number (CFL condition). The default CFL conditions is 0.7, and a higher CFL condition will reduce computational time, but increase potential numerical instabilities. Results show that all CFL conditions smaller than 1 results in similar model accuracy (less than 10% deviation), but computational time decreases by a factor 1.5.

4 *Will a single-precision approach reduce computational expense?*

For the fourth approach, compiling XBeach with single-precision format instead of the current double-precision format, the reduction in computational time is negligible.

8.2 Recommendations for BOI

- The model settings and approaches found in this study are not yet the recommended set for the dune safety assessment of 2023. Here, the potential effect of the approaches on the computational expense is investigated, assuming that a 10% loss in consistency is acceptable. The optimum set will be examined in Phase 2 of the project, during the development of the semi-probabilistic model. Close collaboration and discussion with end-users will be crucial in the following phases of the BOI Zandige Keringen project to ensure the safety assessment remains manageable.
- In the Chapter 7, the impact of the combined measures is quantified by applying a *morfac* of 4. This is a relatively conservative value that was chosen by the authors to have little effect on the consistency of model predictions of dune erosion. This value is therefore not a recommendation by the authors for the dune safety assessment 2023. The relation between the speed-up factor and model accuracy for varying *morfac* values, as presented in this report, shows that the *morfac* can be used in the development of the semi-probabilistic methodology in the next phase within the overall project. For example, an option is to start calculations with a high *morfac* (i.e. small computational efforts). For the profiles where a high probability of failure is predicted, restart the calculations with a lower *morfac* to assure that the predicted failure is not a *morfac*-induced artefact.

- For all simulations within this study two types of boundary conditions are applied; a 6 h simulation period with constant (maximum) wave and surge conditions or a 32 h simulation period with time-varying wave and surge conditions. The effect of both boundary conditions on the resulting morphological change in the model are, on average, comparable. This observation could be useful in the derivation of the semi-probabilistic model in the next phase of the BOI project.

9 References

- Arcadis (2020), BOI Zandige Keringen - Selectie representatieve kustprofielen (werkdocument). C06041.000050.0100
- Deltares (2014), rapport nummer 1209436-002. XBeach 1D – Probabilistic model ADIS, Settings, Model uncertainty and Graphical User Interface. Authors: Pieter van Geer, Joost den Bieman, Bas Hoonhout, Marien Boers.
- Deltares (2015). Achtergronddocument toetschema duinafslag: Filterregels bij toepassing van de gedetailleerde toets duinafslag WTI2017. Deltares rapport 1220085-006, september 2015. Author: M. Boers.
- Deltares (2016). Hydraulische Belastingen 2017 voor Duinwaterkeringen. Deltares rapport 1220083-004-HYE-0003. Author: Joost den Bieman.
- Deltares/Arcadis (2019a). Plan van Aanpak Vernieuwd Instrumentarium Zandige Keringen. Tech. Report 11203720-014-GEO-0001. Authors: R. McCall, R. van Santen, H. Steetzel, A. van Dongeren.
- Deltares/Arcadis (2019b). Vervolgstudie XBeach. Deltares Rapport 11203720-013. Authors: R. McCall, R. van Santen, H. Steetzel, M. de Ridder, A. van Dongeren
- Deltares, (2020a). 'Wave spreading and sediment size effects in the XBeach model', Deltares final report, 11203720-030-GEO-0002, March 2020. Authors: Robert McCall, Ellen Quataert, Anouk de Bakker, Menno de Ridder, Robbin van Santen and Henk Steetzel.
- Deltares (2020b). XBeach BOI Default settings - Calibration of the XBeach model parameters (In Dutch). Deltares Rapport 11205758-029-GEO-0009. Authors: A. De Bakker, R. de Goede, L. de Vet, M. de Ridder, M. van der Lugt, R. McCall, D. Roelvink.
- Deltares (2020c). Boundary condition guidelines for XBeach simulations. Deltares Rapport 11205758-029-GEO-0003. Authors: A. De Bakker, M. de Ridder, R. McCall, A. van Dongeren.
- Expertise Netwerk Waterveiligheid/ENW (2007). TRDA2006 Duinafslag, Technisch Rapport Beoordeling van de veiligheid van duinen als waterkering ten behoeve van Voorschrift Toetsen op Veiligheid.
- Klopman, G., and Dingemans, M. W. (2001). Wave interactions in the coastal zone. International Workshop on Water Waves and Floating Bodies.
- Technische Adviescommissie voor de Waterkeringen/TAW (1984). Leidraad voor de beoordeling van de veiligheid van duinen als waterkering.
- Roelvink, J.A., Reniers, A., Van Dongeren, A.P., De Vries, J.V.T., McCall, R. and Lescinski, J. (2009). Modelling storm impacts on beaches, dunes and barrier islands. Coastal engineering, 56(11-12), pp.1133-1152.

- Rijkswaterstaat (2020). BOI Zandige Keringen Fase 0. Werkdocument: Voorstel definitie faalfunctie en achtergrond faalfunctie beoordelingsmethodiek. Authors: H. Steetzel, R. van Santen, R. McCall, F. Diermanse and J. den Bieman (in Dutch).
- WL | Delft Hydraulics (1982), Computational model for the estimation of dune erosion during storm surge. (Rekenmodel voor de verwachting van duinafslag tijdens stormvloed.) WL | Delft Hydraulics report M1263 part 4 (in Dutch).

A Sensitivity to random seeding of boundary conditions

This appendix provides tables and figures to illustrate the statements made in the main report (section 2.6 and section 4.3.1).

Constant boundary conditions

Table 9-1: Absolute dune erosion volumes based on 100 simulations with constant boundary conditions

	Erosion volumes in m ³					
	Mean	Max	Perc-90	Median	Perc-10	Min
NL, Tp = 12s	-113,25	-115,87	-114,65	-113,46	-111,68	-109,47
NL, Tp = 19s	-184,80	-191,43	-187,91	-184,85	-181,94	-178,95
Wad, Tp = 12s	-57,62	-59,02	-58,43	-57,67	-56,74	-56,47
Wad, Tp = 19s	-82,13	-85,29	-84,26	-82,14	-80,43	-77,76

Table 9-2: Relative variation in dune erosion volume with respect to the mean of 100 simulations with constant boundary conditions.

	Relative erosion volumes with respect to mean erosion volume				
	Max	Perc-90	Median	Perc-10	Min
NL, Tp = 12s	2,32%	1,24%	0,19%	-1,39%	-3,34%
NL, Tp = 19s	3,59%	1,68%	0,02%	-1,55%	-3,17%
Wad, Tp = 12s	2,43%	1,41%	0,10%	-1,53%	-1,98%
Wad, Tp = 19s	3,84%	2,59%	0,02%	-2,07%	-5,32%

Time-varying boundary conditions

Table 9-3: Absolute dune erosion volumes based on 10 simulations with time-varying boundary conditions.

	Erosion volumes in m ³			
	Mean	Max	Median	Min
NL, Tp = 12s	-110,04	-110,71	-110,07	-108,59
NL, Tp = 19s	-200,38	-203,22	-200,33	-197,36
Wad, Tp = 12s	-45,57	-46,50	-45,50	-44,62
Wad, Tp = 19s	-56,24	-58,27	-56,14	-54,35

Table 9-4: Relative variation in dune erosion volume with respect to the mean of 10 simulations with time-varying boundary conditions.

	Relative erosion volumes with respect to mean		
	Max	Median	Min
NL, Tp = 12s	0,61%	0,03%	-1,32%
NL, Tp = 19s	1,42%	-0,03%	-1,51%
Wad, Tp = 12s	2,03%	-0,15%	-2,08%
Wad, Tp = 19s	3,60%	-0,19%	-3,37%

Figure A-9-1 illustrates the increasing spread in predicted erosion volumes, and hence increasing uncertainty, due to random wave seeding. The 70% confidence interval is used as a measure for the bandwidth of predicted erosion volumes over 10 similar simulations with equal conditions, but different random wave seeding. The figure shows that this bandwidth increases for increasing morfac. Since similar results are found for simulations with constant and time-varying boundary conditions, only the results with time-varying conditions is presented here.

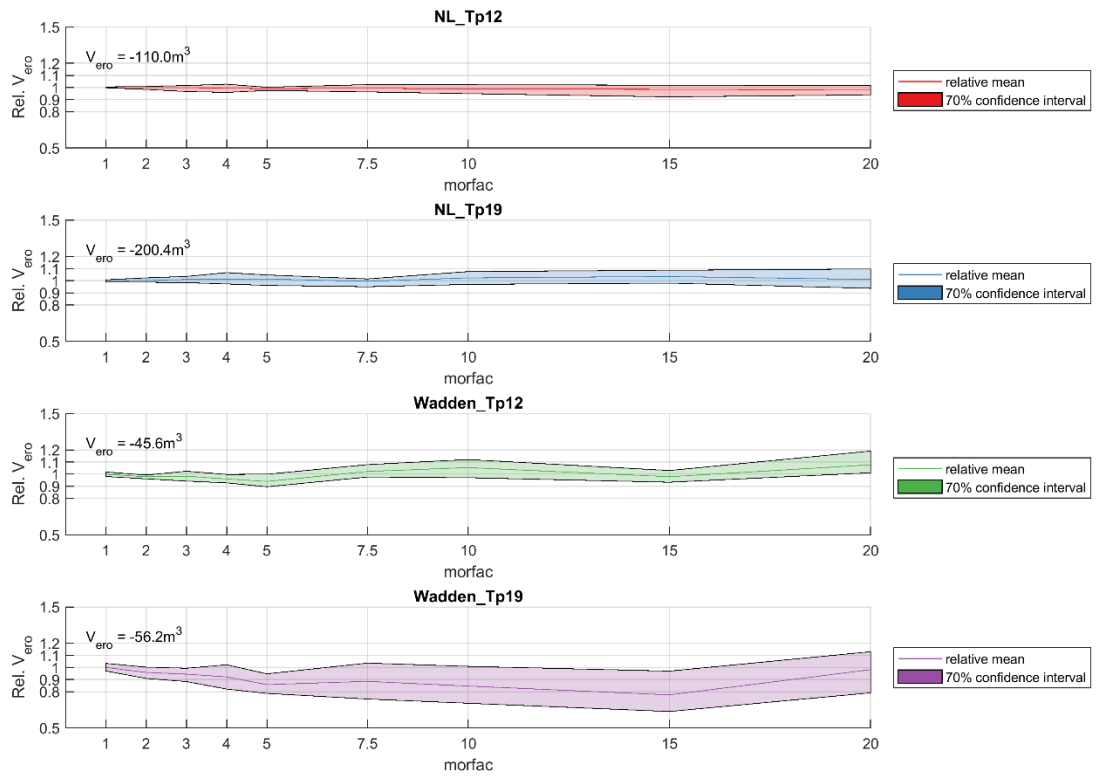


Figure A-9-1: Relative erosion volumes with respect to the mean erosion volume found in 10 simulations with morfac=1, for 10 simulations with time-varying boundary conditions per different morfac value. The bandwidth (represented with the 70% confidence interval) of erosion volumes increases for increasing morfac, indicating the increase in uncertainty due to random wave seeding.

B Statistical measures

In this report multiple statistical measures are applied to interpret the results. The definitions of these statistical measure are given in this appendix. The following statistical measures are applied in this report:

- Mean:

$$\text{mean} = \langle y \rangle \quad (0.7)$$

where y is list of values.

- Standard deviation:

$$\text{STD} = \sqrt{\langle (y - \langle y \rangle)^2 \rangle} \quad (0.8)$$

where y is list of values.

- Relative bias:

$$\text{rel. bias} = \frac{\langle y - \hat{y} \rangle}{\sum \hat{y}} \quad (0.9)$$

where y is the computed value and \hat{y} the observed value.

- Scatter index:

$$\text{SCI} = \frac{\sqrt{\langle (y - \hat{y})^2 \rangle}}{\langle \hat{y} \rangle} \quad (0.10)$$

where y is the computed value and \hat{y} the observed value.

C Supplementary document with figures

The results of all the 26 profiles for the different reduction methods are shown in a supplementary document. This document compares variations in each reduction approach against the base case for all the profiles.

Deltares is an independent institute for applied research in the field of water and subsurface. Throughout the world, we work on smart solutions for people, environment and society.

Deltares

www.deltares.nl